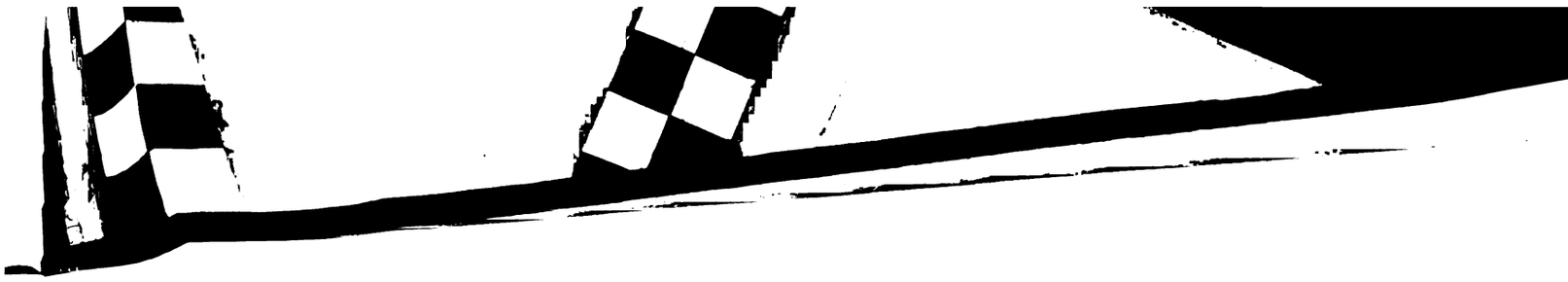

ABSTRACT

THE USE OF HEMODIALYSIS
IN THE STUDY OF THE LOCAL VASCULAR
EFFECTS OF POTASSIUM DEPLETION

By

Steven A. Roth

Only a fraction of the cardiac output is received by each of the many parallel components in the systemic circulation. The distribution of the cardiac output among these competing systemic organs depends upon their relative resistance to blood flow. The cations H^+, K^+, Mg^{++}, and Ca^{++} are known to participate in the control of vascular resistance by actively changing the calibre of the arterioles, the resistance controlling vessels. The effects of ions upon the cardiovascular system are of interest because electrolyte concentration in blood and blood vessel wall is abnormal in some types of experimental and naturally occurring hypertension and hypotension. Most diseases which produce hypertension also alter electrolyte concentration in blood and tissue. Furthermore, the alterations in blood electrolyte concentration are rather consistent between those diseases which are accompanied by hypertension.

The objectives of this study were to determine the effects of abnormally low plasma potassium concentrations, that is, hypokalemia, upon vascular resistance and to mathematically describe the transport of potassium between the various vascular compartments.

Steven A. Roth

The acute response to hypokalemia was measured by interposing a hemodialyzer in the arterial supply of the collateral-free gracilis muscle of the dog. Blood flow was held constant while measuring perfusion pressure. During the control period, the blood was dialyzed against a Ringer's solution designed to have little effect on plasma ion concentrations. In the experimental phase, the blood was dialyzed against Ringer's solution lacking potassium ion, producing arterial plasma potassium concentrations considerably lower than the normal value of 4 meq/l.

Two models for the transport of potassium in skeletal muscle were studied by means of a series of potassium depletion experiments. The muscle was considered to be made up of "compartments" consisting of plasma, interstitial fluid, and intracellular fluid. The simpler model consisted of two perfectly mixed compartments, a combined plasma and interstitial compartment and an intracellular compartment. The other model separated plasma and interstitial fluid and considered the concentration gradient along the capillary in the flow direction.

The findings of this study were that the acute local vascular response to hypokalemia as produced by a non-dilutional technique was constriction and increased vascular resistance. Furthermore, the relationship between percent change in plasma potassium concentration and percent change in vascular resistance appeared to be linear,

resistance increasing about 12½% for a 50% reduction in potassium ion concentration.

Both the two- and three-compartment models were adequate for describing potassium transport in skeletal muscle. The two-compartment model neglected the resistance to mass transfer across the capillary wall and, hence, predicted somewhat higher rates of mass transfer. Both models indicated that the acute response is accompanied by a rapid decrease in the interstitial concentration of potassium, followed by the gradual reduction of potassium concentration in skeletal muscle cells.

THE USE OF HEMODIALYSIS IN THE STUDY OF THE LOCAL VASCULAR EFFECTS OF POTASSIUM DEPLETION

By

Steven A. Roth

A THESIS

Submitted to
Michigan State University
in partial fulfillment of the requirements
for the degree of

DOCTOR OF PHILOSOPHY

Department of Chemical Engineering

1970

To my wife and parents

ACKNOWLEDGMENTS

The author wishes to express his sincere appreciation to his advisor, Dr. D. K. Anderson, whose guidance and assistance were invaluable throughout the course of this study. Thanks are also due the other members of the author's guidance committee: Dr. M. H. Chetrick, Dr. G. A. Coulman, Dr. J. B. Scott, and Dr. L. F. Wolterink.

The author is indebted to the National Science Foundation for providing financial support.

Appreciation is also extended to Mr. C. M. Redman for constructing the test apparatus used in this study.

TABLE OF CONTENTS

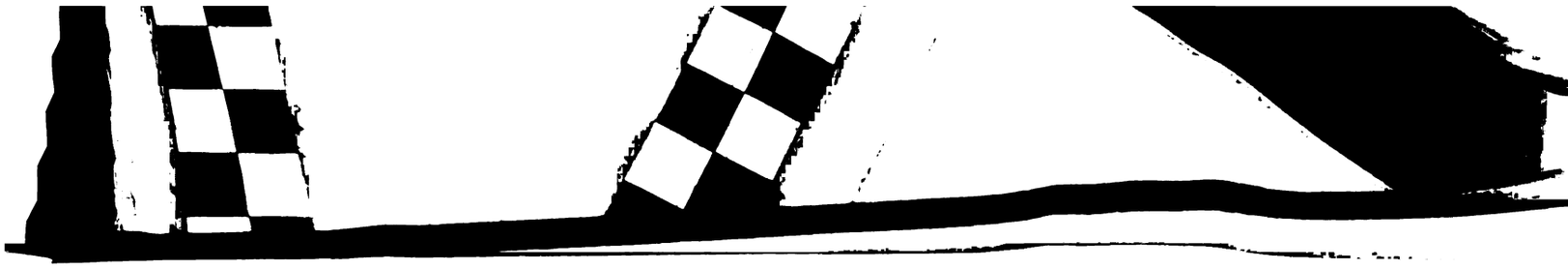

LIST OF FIGURES

LIST OF TABLES

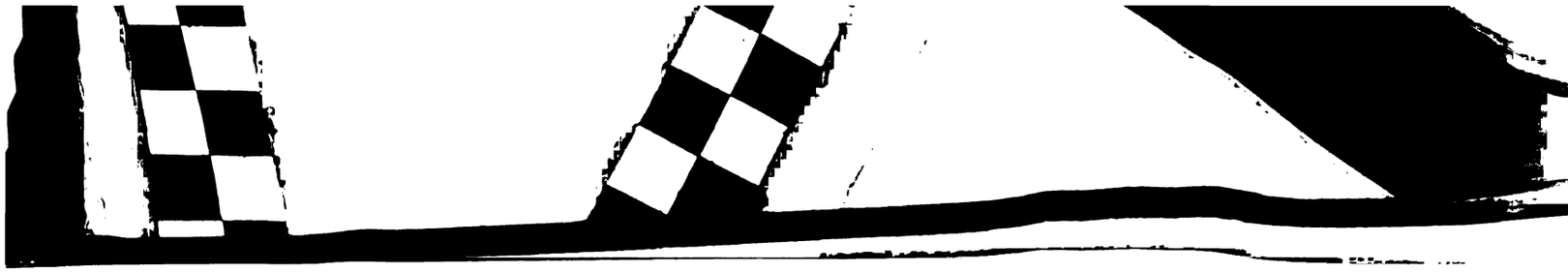

INTRODUCTION

Only a fraction of the cardiac output is received by each of the many parallel components in the systemic circulation. The distribution of the cardiac output among these competing systemic organs depends upon their relative resistance to blood flow. A simplified description of the circulation is given in Figure 1. Each of the main circulatory paths contains many elements in series. Blood flows successively through the main arteries, small arteries, arterioles, and capillaries to the venous or low-pressure side of the circulation. Each element in the series actually consists of many similar vessels in parallel so that the total cross-sectional area for flow increases as the capillaries are approached.

The smooth muscle in the walls of the arterioles gives these vessels the capability to change calibre and thus alter blood flow. The laminar flow of a Newtonian fluid through a cylindrical tube may be described by the Hagen-Poiseuille equation,

$$\Delta P/Q = R = (8/\pi)x(\mu)x(\ell/r^4). \qquad (1)$$

Thus, resistance is the product of a numerical coefficient, a viscous component, and a geometric component. If this equation can be applied to the circulation of blood and if blood viscosity can be considered constant, then the relative resistances to flow in the various vascular beds

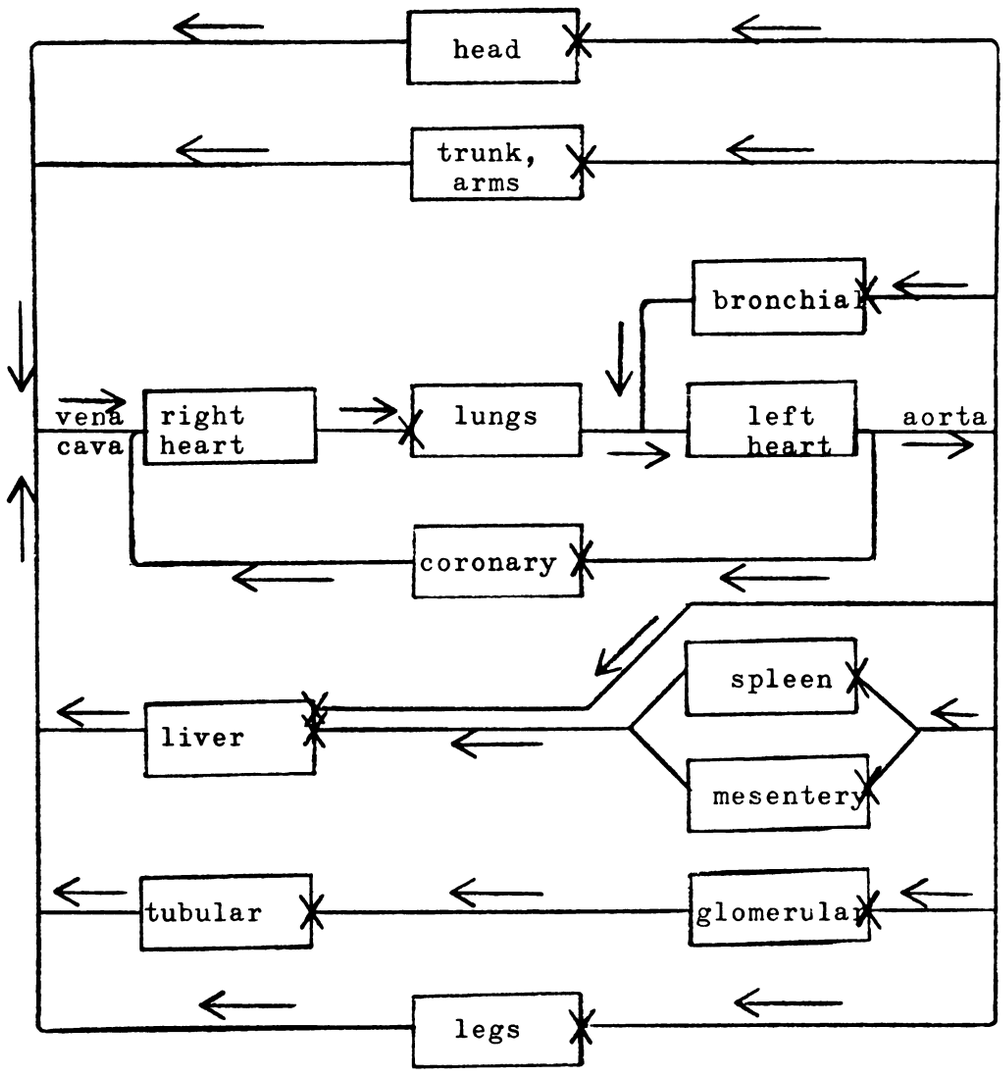

X = flow control point

Figure 1. A Simplified Diagram of the Mammalian Circulatory System[9]

can be determined by comparing the quantities $(1/N)x(\ell/r^4)$, where N is the number of capillaries in parallel.

The determinants of the vascular resistance are shown in Figure 2. As predicted by the Hagen-Poiseuille equation, resistance is immediately determined by a geometric component, ℓ/r^4, and a viscous component, μ. Changes in vessel length are not ordinarily seen, except perhaps in the lung. Hence, vessel radius is the most important variable in the geometric component of resistance. It is influenced by the contractile state of vascular smooth muscle, transmural pressure, and morphological changes in the vessel wall.

Many naturally occurring chemical agents in blood influence the function of the heart and blood vessels, including the major cations in plasma, H^+, K^+, Mg^{++}, and Ca^{++}. The effects of ions upon the cardiovascular system are of interest because electrolyte concentration in blood and blood vessel wall is abnormal in some types of experimental and naturally occurring hypertension and hypotension. Most diseases which produce hypertension also alter electrolyte concentration in blood and tissue. Furthermore, the alterations in blood electrolyte concentrations are rather consistent between those diseases which are accompanied by hypertension. In addition, the ions may play a role in the local control of blood flow, both in normal and abnormal physiology.

The experimental manipulation of the ionic concentration of extracellular fluid by a direct method such as the

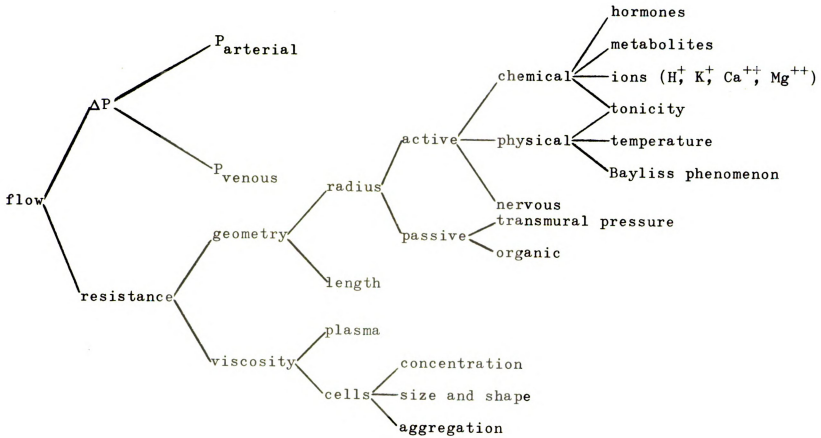

Figure 2. The Determinants of Resistance[23]

infusion of various artificial solutions into the blood, undoubtedly alters the ionic concentration of the cells, including the smooth muscle cells of the blood vessel wall which are the site of the vasoactive machinery. Thus, a description of the resistance controlling mechanism must consider changes in intracellular ionic composition.

The objectives of the present study are (1) to determine the effects of abnormally low plasma potassium concentrations, i.e., hypokalemia, upon vascular resistance in skeletal muscle and (2) to develop a mathematical description of the distribution and exchange of potassium between the various vascular compartments of skeletal muscle. Such information should be helpful in understanding the resistance controlling mechanism.

BACKGROUND

This section will summarize the work of other investigators which is pertinent to this study. Included in this section are: (A) the known vascular effects of the cations, (B) the previous experimental technique for studying low plasma ion concentrations, (C) the experimental technique, dialysis, used in this study, and (D) mathematical models simulating the transport of various substances through the circulatory system.

The Acute Vascular Effects of the Cations

The acute vascular effects of the cations have been summarized[20,21,22,23] and will be reviewed here. The potassium ion is of particular interest since it appears to be the most vasoactive monovalent cation and has three distinct actions on the peripheral vascular system. Elevation of the plasma potassium concentration to levels less than twice the normal value of 4 meq/l produces arteriolar dilation, while the acute local effect of a large excess of plasma potassium (greater than approximately 14 meq/l) is constriction. Lower than normal potassium concentrations, as produced by a dilutional technique, result in constriction and increased vascular resistance.

Calcium is the only ion thus far studied which acts as a constrictor in most vascular beds when the local concentration is elevated above the normal range occurring in life. The acute local effect of a plasma calcium deficit appears

to be dilation.

Moderate excesses of Mg^{++} or H^{+} in the blood produce the acute local effect of dilation. The acute local effect of a blood hydrogen ion deficit is constriction while the reduction of plasma magnesium concentration by itself has no effect upon resistance to flow unless it is combined with other ionic abnormalities.

Because plasma sodium concentration cannot be significantly increased without increasing plasma tonicity as well, it is difficult to study the specific acute local vascular action of the sodium ion. The available evidence suggests, however, that there are no actions which are characteristic of the sodium ion.

Experimental Techniques

In a physiological experiment where both driving pressure (arterial pressure minus venous pressure) and volume flow are known, the resistance to flow can be calculated and compared with the resistance to flow under other conditions. If blood viscosity can be assumed constant, then a comparison of resistances is sufficient to conclude, without doubt, whether the vascular bed of concern has constricted or dilated. However, the reason for the change in resistance will not be revealed without careful examination of the experiment. As shown in Figure 2, the reason for the change in resistance might be active or passive in origin.

The reduction of ion concentrations presents difficulties. Possible direct methods include electrodialysis, dialysis, fixed bed processes, ultrafiltration with fluid replacement, and dilution. Dilution, of course, does not remove solutes from blood, it simply reduces their concentration.

This technique was used in a study by Haddy et al.[21] to transiently render hypokalemic (1.9 meq/l), alkalotic (pH 7.54), hypercalcemic (6.4 to 13.5 meq/l), hypomagnesemic (1.2 meq/l), and hypocalcemic (3.0 meq/l) the blood flowing through the vascular beds of the dog forelimb, kidney, and heart. Resistance to flow was measured by holding the flow rate constant and measuring the effects of rapid intra-arterial infusion of the artificial solution upon the perfusion pressure. Their conclusion was that more marked constriction occurs with combinations of local hypokalemia, hypercalcemia, alkalosis, and hypomagnesemia than with any one of the abnormalities alone.

Dilution, of course, alters hematocrit, viscosity, and probably the proportion of free and bound ion concentrations. The change in the geometric component of resistance is superimposed upon the change in the viscous component. All changes must be referenced against a control infusate which has little effect upon plasma Na^+, K^+, Ca^{++}, Mg^{++}, and HCO_3^-, and yet which dilutes the blood cells, plasma proteins, and organic substances to the same degree as the infusions designed to alter ionic concentrations.

Hemodialysis

Hemodialysis may be defined as the passive equilibration of blood with a dialyzing fluid by diffusion through a membrane. Because it is so closely associated with the artificial kidney, the two terms are often used interchangeably. But the emphasis which has been placed upon hemodialysis as a treatment for uremic patients, tends to obscure the fact that blood can be treated in an extracorporeal circuit for a variety of purposes related to research. Indeed, when the first hemodialysis was performed (in a laboratory of pharmacology) the process was envisioned as a research tool.[1]

All artificial kidneys, or hemodialyzers, now in clinical use are based upon the principle of diffusion through a cellulose membrane. Artificial kidney is a misnomer, since a hemodialyzer is incapable of duplicating the functions of the normal kidney. However, it does have the ability to remove water and a variety of metabolites and poisons, to regulate several ions, and to adjust pH. Optimization of the artificial kidney, even on the basis of this restricted performance, is not possible at this time, largely because of the inability to define what constitutes satisfactory rehabilitation and to relate it to operating conditions.

Two types of hemodialyzers have been widely accepted for clinical application. In the tubular dialyzer, blood

Hemodialysis

Hemodialysis may be defined as the passive equilibration of blood with a dialyzing fluid by diffusion through a membrane. Because it is so closely associated with the artificial kidney, the two terms are often used interchangeably. But the emphasis which has been placed upon hemodialysis as a treatment for uremic patients, tends to obscure the fact that blood can be treated in an extracorporeal circuit for a variety of purposes related to research. Indeed, when the first hemodialysis was performed (in a laboratory of pharmacology) the process was envisioned as a research tool.[1]

All artificial kidneys, or hemodialyzers, now in clinical use are based upon the principle of diffusion through a cellulose membrane. Artificial kidney is a misnomer, since a hemodialyzer is incapable of duplicating the functions of the normal kidney. However, it does have the ability to remove water and a variety of metabolites and poisons, to regulate several ions, and to adjust pH. Optimization of the artificial kidney, even on the basis of this restricted performance, is not possible at this time, largely because of the inability to define what constitutes satisfactory rehabilitation and to relate it to operating conditions.

Two types of hemodialyzers have been widely accepted for clinical application. In the tubular dialyzer, blood

flows through a coil of cellulose membranes which are bathed in a dialysate fluid. In the parallel-plate dialyzer, blood flows between two parallel walls that are permeable to blood solutes. The latter is the dialyzer design used exclusively in this study and it will be discussed in detail.

The problem is illustrated in Figure 3. Blood, or the "blood" side fluid, flows between two parallel walls which can be considered to be of infinite width. At a certain point the fluid contacts the section of the wall that is permeable. The flow is laminar and fully developed before the fluid contacts this section of the channel. A dialysate fluid flows on the other side of the permeable wall. Its flow rate is high enough compared to the blood flow rate to consider its concentration to be zero at all points.

Grimsrud and Babb[13,16] solved the partial differential equation describing the steady-state transfer of a solute from blood in a parallel-plate dialyzer. The governing equation

$$\partial^2 C^*/\partial y^{*2} = 3/2(1 - y^{*2})\,\partial C^*/\partial x^* \qquad (2)$$

is derived by considering convective mass transfer in the flow direction and mass transfer by diffusion in the direction perpendicular to flow. The partial differential equation can be solved by separation of variables to yield the concentration at any point in the channel. This solution can then be integrated over the cross section of the channel

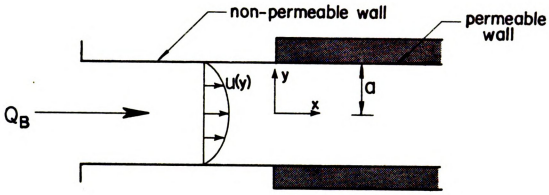

$$\frac{\partial^2 C^*}{\partial y^{*2}} = \frac{3}{2}(1-y^*)\frac{\partial C^*}{\partial x^*}$$

where: $x^* = \frac{x\mathcal{D}}{ua^2}$ & $C^* = \frac{C_B}{C_{Bi}}$

$y^* = \frac{y}{a}$

B.C.'s: at $x^*=0$, $C^*=1$ for all y^*

at $y^*=0$, $\frac{\partial C^*}{\partial y^*}=0$ for all x^*

at $y^*=1$, $C^* = -\frac{\mathcal{D}}{Pa}\frac{\partial C^*}{\partial y^*}\Big|_{y^*=1}$ for all x^*

Figure 3. Parallel-Plate Dialysis: The Steady State Problem

using the velocity as a weighting function to obtain the bulk concentration as a function of the flow direction. An overall mass transfer coefficient can be defined as

$$h_o = -(Q_B/2wC_B)dC_B/dx. \qquad (3)$$

Thus, the solution for the bulk concentration as a function of distance down the dialyzer enables investigating the behavior of the overall mass transfer coefficient along the direction of flow. The important conclusion which can be drawn from such a solution is that for small values of the wall Sherwood number, $Pa/\mathcal{D}$, the overall mass transfer coefficient is a constant independent of the dialyzer length.[13] At first consideration this would appear to be a reasonable conclusion since the wall Sherwood number is simply the ratio of the membrane permeability and the equivalent fluid permeability for diffusion through a stagnant film of thickness a. When membrane resistance is controlling, h_o is constant along the length of the dialyzer.

Van der Does de Bye and Schenk[36] studied the corresponding problem in heat transfer. They solved the problem, in which heat is transferred from a fluid flowing in laminar flow between two parallel plates. The plates had a finite resistance to heat transfer and the temperature on the outside of the plates was held constant. A solution to the problem was obtained for two values of the wall Nusselt number, ha/k, of 1 and 10.

The performance of hemodialyzers can be described by

$$Q_B(C_{Bi} - C_{Bo}) = h_o A(C_{Bi} - C_{Bo})/\ln(C_{Bi}/C_{Bo}). \quad (4)$$

It has been assumed that C_{Di} and C_{Do} are both zero due to the much higher dialysate flow rate than blood flow rate. This equation has been optimized by Grimsrud and Babb[14] subject to two constraints, (1) the blood volume or priming volume of the dialyzer must not exceed some maximum value, that is,

$$2aw\ell \leq V_{max} \quad (5)$$

and (2) the pressure drop must not exceed some maximum value, that is,

$$3\mu\ell Q_B/2wa^3 \leq \Delta P_{max}. \quad (6)$$

Maximizing the mass transfer rate with respect to the half channel height, a, yields the design equation recommended for calculating the optimum membrane spacing

$$a = 1.6\sqrt[3]{h_o \mu \ell^2/\Delta P_{max}}. \quad (7)$$

The resistance to mass transfer, $1/h_o$, is the sum of three resistances in series, blood, membrane, and dialysate, so that

$$1/h_o = R_T = R_B + R_M + R_D. \quad (8)$$

R_D may be neglected on the grounds of turbulent dialysate

flow,[2] R_M is the reciprocal of the membrane permeability, $1/P$, and R_B has been shown to equal $0.5a/\mathcal{D}$.[2] Thus,

$$1/h_o = 1/P + 0.5a/\mathcal{D}. \qquad (9)$$

Since h_o is a function of a, the solution of the equation for the optimum value of the half channel height requires trial and error.

Several interesting results can be derived from this optimization.[14] Among these are: (1) for a given dialyzer length, there is one, and only one height that will produce a maximum value of mass transfer rate, (2) this maximum peak on the plot of transfer rate versus half channel height is sharp, indicating the importance of being able to maintain the height of the blood channel to within narrow limits, and (3) the shorter the dialyzer, the higher the value of the optimum mass transfer rate.

The latter result is true since, subject to the constraints given by (5) and (6), a shorter dialyzer permits a larger flow rate, Q_B, a smaller half channel height, a, a higher value of the overall mass transfer coefficient, h_o, and a larger area for mass transfer, $2w\ell$. Of course, there are practical limitations as to how short the dialyzer can be made.

Having recognized the importance of the design variable a, it next remains to investigate means to closely control the thickness of the blood film. The most common parallel-plate hemodialyzer in clinical use is the Kiil dialyzer.

This design utilizes a notched membrane support as illustrated in Figure 4.

(a) in theory (b) in actual use

Figure 4. The Kiil Membrane Support

The major disadvantages of this support system are that it limits dialysate flow to the laminar regime, making it necessary to consider the resistance to mass transfer on the dialysate side, and it permits the membrane to sag. Under typical operating conditions, the blood volume in the Kiil dialyzer is 4 to 6 times that predicted on the basis of the nominal membrane separation.[15] This is an obviously inadequate means of membrane support, if one is interested in optimizing dialyzer design and performance.

Babb and Grimsrud[15] have proposed the use of foam nickel metal as a membrane support and have been able to construct test dialyzers which approach theoretical performance.[13,16] The nickel foam found most useful has interconnected pores and a nominal density of 3% of the solid nickel. Its advantages over the Kiil support are many. It virtually eliminates membrane sag, promotes dialysate mixing, does not screen the membrane, and does not limit

dialysate flow rate by pressure drop. Because it represents a means of constructing highly efficient dialyzers, the foam nickel membrane support was used for the dialyzers in this study. However, nickel foam is not without its disadvantages as will be discussed later.

Transport Models for the Circulatory System

The need for adequate mathematical models simulating the transport of various substances through the circulatory system has been recognized as being of scientific interest for physiology as well as having great practical interest in pharmacology. Blood is readily accessible to sampling and measurement, but the actual site of drug action or chemical toxicity is more likely to be located elsewhere than in the bloodstream, for example, the central nervous system. If transport between the critical region and blood stream is not rapid enough, a device which simply removes the drug or metabolite from the blood will serve little purpose. This has particular implications to hemodialysis. The observation that the concentration of urea rises more rapidly after dialysis than can reasonably be predicted on the basis of metabolism alone, the "rebound phenomenon," indicates that large quantities of solute remain stored in other compartments of the body. A careful simulation must account for both the initial distribution of each solute and its intercompartmental exchange rate.

Bischoff and Brown[6] have summarized various simplified models which can be used to describe a local region as well as various possible arrangements for assembling local regions to simulate a simplified mammal. Compartments can be defined in terms of body fluids, body tissues, or a combination of both. The body's vascular compartments are treated as separate homogeneous pools even though fluids are distributed throughout the body in a heterogeneous manner.

Vadot[35] used this approach and presented solutions for mass transfer between two, three, and four perfectly mixed compartments separated by semi-permeable membranes. This model (see Figure 5) may be thought of as dialysis in series.

Bell, Curtis, and Babb[4] have successfully used a two-compartment model to simulate plasma urea and creatinine concentration variations in uremic patients undergoing intermittent dialysis. A two-compartment model has the advantage of requiring only one mass transfer coefficient. The model is illustrated in Figure 5. The product of the mass transfer coefficient and the transfer area, $k_c A_c$, was varied to obtain a best fit of the data from each patient.

Dedrick and Bischoff[10] have modeled barbiturate distribution using a four-compartment model consisting of a blood pool, viscera, lean tissue, and adipose tissue as shown in Figure 5. Intercompartmental transport between the homogeneous compartments takes place by flow only, rather than by diffusion only as in the previous models, with all metabolism confined to the viscera. Equilibrium concentrations

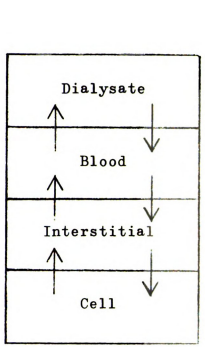

(a) Vadot[35]

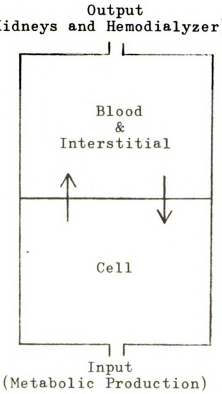

(b) Bell, Curtis, Babb[4]

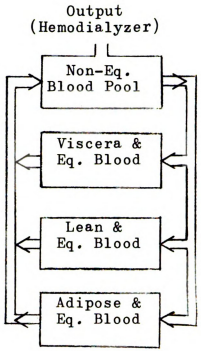

(c) Dedrick, Bischoff[10]

Figure 5. Some Typical Transport Models with Hemodialysis
(⟶ = Transport by Diffusion, ⟹ = Transport by Flow)

are a function only of free concentration in each compartment. The effect of hemodialysis on drug distribution was studied by assuming an artificial kidney with constant clearance, while drug distribution without hemodialysis was studied by considering the artificial kidney to have zero clearance. Clearance is defined as the quantity

$$\text{Clearance} = Q_B(C_{Bi} - C_{Bo})/C_{Bi}, \qquad (10)$$

which may be thought of as the volumetric flow rate of blood through the dialyzer, measured in ml/min, which is completely cleared of solute. It tends to be rather constant since the lower the blood flow rate, the greater the decrease in solute concentration across the dialyzer. Clearance must, of course, be expressed in terms of a particular solute. The clinical performance of dialyzers is usually measured with respect to the removal of urea, which is a symbolic rather than a demonstrably controlling solute.

The results from the model of Dedrick and Bischoff predict the "rebound" phenomenon in the blood pool and the well perfused viscera. When dialysis is terminated, the original drug distribution is reversed and the drug moves from the poorly perfused tissues into the blood pool and viscera.

THEORY

The surgical procedure for studying the acute response to hypokalemia has been developed by Haddy and co-workers[33] and was adapted for this study. However, concentration changes were achieved by using a hemodialyzer rather than a dilutional technique. A hemodialyzer was interposed in the arterial supply of the collateral-free gracilis muscle. When blood flow is held constant, changes in resistance to flow are indicated by changes in perfusion pressure. Thus, the vascular response to various degrees of hypokalemia can be calculated by continuously monitoring perfusion pressure referenced to a control.

Any consideration of the transport of potassium in skeletal muscle must consider the three body fluids; blood, interstitial fluid, and intracellular fluid, separately or in combination. Two of the simplified models suggested by Bischoff and Brown[6] appear to be applicable. They are shown together with the appropriate equations in Figure 6. The combination of the intracellular fluid with any other fluid compartment is unreasonable because of the existence of potential and concentration gradients across the cell wall. Only similar compartments should be lumped together.

The three-compartment model is similar to that used by Bellman, Kalaba, and Jacquez[5] to model drug distribution in a one organ entity following its injection into the blood stream. Tracer studies with K^{42} have shown that the uptake

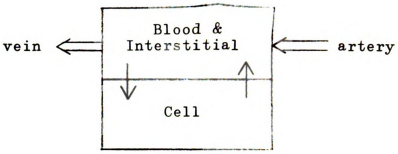

Blood/Interstitial Compartment:

$$\frac{dC_{B,i}}{dt} = \frac{(1 - Hct)Q_B}{V_B(1 - Hct) + V_i}(C_{art} - C_{B,i}) + \frac{k_c A_c}{V_B(1 - Hct) + V_i}\left(\frac{C_c}{m} - \frac{b}{m} - C_{B,i}\right).$$

Intracellular Compartment:

$$\frac{dC_c}{dt} = \frac{k_c A_c}{V_c}\left(C_{B,i} + \frac{b}{m} - \frac{C_c}{m}\right).$$

(a) Two-Compartment Model

Figure 6. Possible Models for Potassium Transport in Skeletal Muscle

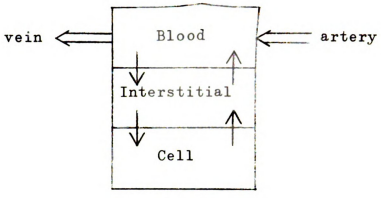

Blood Compartment:

$$\frac{\partial C_B}{\partial t} + \frac{Q_B \ell}{V_B} \frac{\partial C_B}{\partial x} = \frac{k_B A_B}{V_B(1 - Hct)} (C_i - C_B).$$

Interstitial Compartment:

$$\frac{dC_i}{dt} = \frac{k_B A_B}{V_i} \frac{1}{\ell} \int_0^{\ell} (C_B - C_i)dx + \frac{k_c A_c}{V_i} \left(\frac{C_c}{m} - \frac{b}{m} - C_i\right).$$

Intracellular Compartment:

$$\frac{dC_c}{dt} = \frac{k_c A_c}{V_c} \left(C_i - \frac{C_c}{m} + \frac{b}{m}\right).$$

(b) Three-Compartment Model

Figure 6. Possible Models for Potassium Transport in Skeletal Muscle (cont.)

of K^{42} by dog erythrocytes is extremely slow[12,34] and, hence, a plasma compartment is used in the model rather than a blood compartment. The derivations of these equations and the assumptions are presented in Appendix I, as are the calculation of average values for the coefficients in both models.

The movement of potassium has been considered to be passive with respect to equilibrium conditions which can be described by $C_B = C_i$ and $C_c = mC_i + b$. Active transport terms could be added to the equations describing the interstitial and intracellular compartments if necessary, but this would require an additional mathematical description for this transport mechanism. Values of m and b were obtained from the data summarized by Waddell and Bates[37] for the distribution of potassium in dog skeletal muscle for various treatments and conditions. A least squares fit of the data given for dogs gives m = 18.9 and b = 79.4 meq/l with a coefficient of correlation of 0.91.

APPARATUS

Dialyzers

Two Babb-Grimsrud hemodialyzers were constructed, similar in design except for minor modifications and size. The smaller dialyzer was constructed in the following manner: A 4x4x1/8 inch groove with dialysate headers on each side was milled in the center of a 6x8x1 inch piece of Lucite (refer to Figure 7). A 4x4x1/8 inch piece of nickel foam metal was glued into this groove and the nickel foam and Lucite were milled as a unit to make the Lucite and foam surfaces completely flush. The nickel foam used has a nominal density of 3% of the solid nickel, pore diameter from 0.008 to 0.050 inch, web thickness 0.004 $\pm$ 0.002 inch, and is available commercially from General Electric in several other pore sizes and densities.

Two such Lucite pieces were then placed face to face, and guide pins were inserted so that the dialyzer could always be assembled in the same manner. All sides of the dialyzer were then machined as a unit. Blood headers were made to screw onto each end of the Lucite blocks with rubber gaskets used to insure a good fit. The inlet header was 4x1/4x1/4 inch and the outlet header was 4x1/4x1/8(deep) inch. The outlet header was made more shallow than the inlet header to minimize the holdup volume between the mass transfer area and the blood outlet. The inlet and outlet lengths of two inches in the blood channel were used to

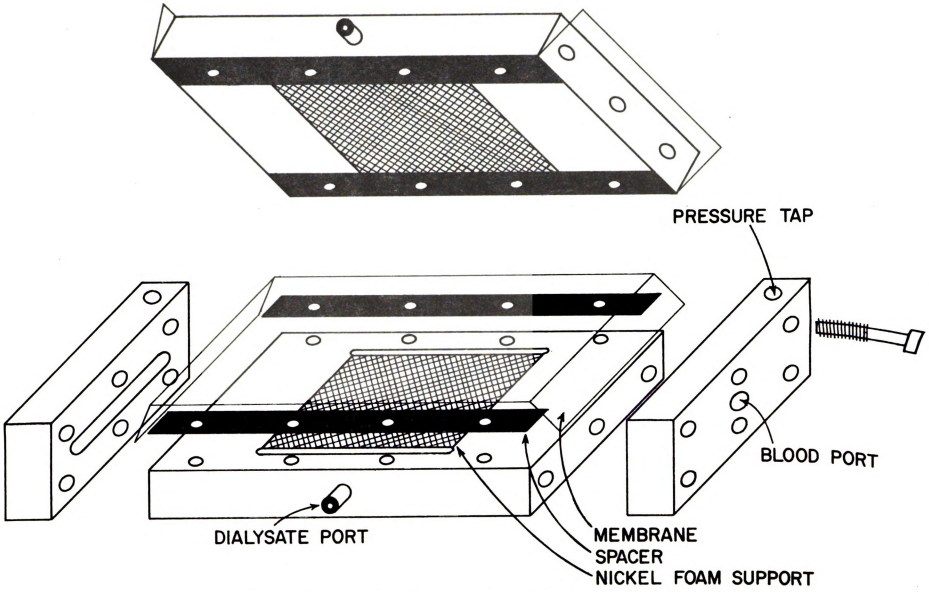

Figure 7. Exploded View of Hemodialyzer

dampen out any header influences.

Stainless steel spacers of various thicknesses were made to control the height of the blood channel. The guide pins also served to align the spacers assuring a leak free assembly.

Dialysis Membranes

Cuprophane PT 150 membranes of regenerated cellulose were used in this study. They have a dry thickness of about 0.5×10^{-3} inch and a wet thickness of about 1.0×10^{-3} inch.[28] Cellulose membranes have negligible ion exchange capacity.[27] These membranes discriminate on the basis of size and shape. Small ions and molecules permeate the membrane with relative ease, transport decreasing as ionic or molecular size increases until a limiting cutoff value is reached.

Dialysate Solutions

Two physiological dialysate solutions were used, a control solution (in g/l, NaCl 7.2, KCl 0.3, $MgCl_2 \cdot 6H_2O$ 0.2, Ca Gluconate 1.0, $NaHCO_3$ 1.9) containing approximately the normal concentrations of the major cations and anions (as compared with blood in Figure 8), and another in which the normal 4 meq/l potassium ion is replaced by sodium ion to maintain a normal osmolarity of about 300 mosm. An osmol is 6.023×10^{23} particles without regard to the species of the particle (as long as it is not water). An ionized substance contributes one particle for every

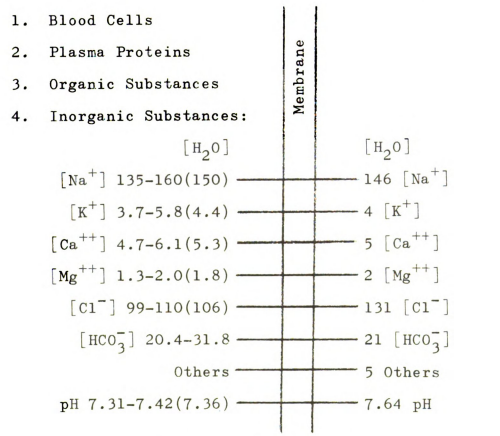

Figure 8. A Comparison of Blood Plasma Composition and Control Dialysate Composition

ion formed in the dissociation of a molecule. Intravenous infusion of such a Ringer's solution for 5 minutes at 10 ml/Kg into the anesthetized dog caused little change in blood pH, plasma osmolarity and plasma sodium, potassium, magnesium, and calcium concentrations.[11] Thus, it is assumed it will have a negligible effect on the above variables when used as a dialysate solution.

Dialysate Supply System

A compact dialysate delivery system was constructed with a maximum capacity for five 2-gallon dialysate containers. Each solution can be delivered to the dialyzer by means of a valving arrangement and dialysate solutions can be changed instantaneously. The pump (Maisch constant metering, Central Scientific Company) can be connected in the flow circuit to push the dialysate through the foam metal membrane support or suck it through, thus offering the choice of positive or negative pressures on the dialysate side. For the in-vivo experiments, the dialysate solutions were kept in a constant temperature water bath at 37°C. Dialysate solution was re-cycled back to its own container. Thus, potassium would build up in the "potassium-free" dialysate fluid over the length of the experiment. The volume of dialysate fluid was sufficiently large to insure that the potassium concentration in the "potassium-free" dialysate never exceeded 10% of the potassium concentration in normal plasma. Dialysate

flow rates were calibrated with a stopwatch and graduated cylinder at the outlet of the return line.

Conductivity Measurements

A series of experiments were conducted to determine the response to a step change in dialysate composition using a continuous flow conductivity cell at the blood outlet and a dilute KCl solution as the "blood" side fluid. The conductivity cell was constructed using Lucite to hold two electrodes made of 1/16 inch diameter stainless steel rod. The electrodes were on opposite sides and flush with a 1/8 inch diameter flow channel. The electrical circuit for measuring and recording concentration as a function of time is shown in Figure 9. The circuit is designed so that the voltage drop across the resistor R is proportional to the reciprocal of the conductivity cell resistance R_c.

The voltage drop across R is $\mathcal{E} = IR$ where

$$I = V/(R_c + R). \tag{11}$$

If R_c is much greater than R, then

$$\mathcal{E} = VR/R_c. \tag{12}$$

Since both V and R are constant, E is proportional to $1/R_c$ for $R_c \gg R$. R is a fixed 1 ohm resistor and R_c is never lower than 10,000 ohms. Therefore, the maximum error which can result from this approximation is 0.01%.

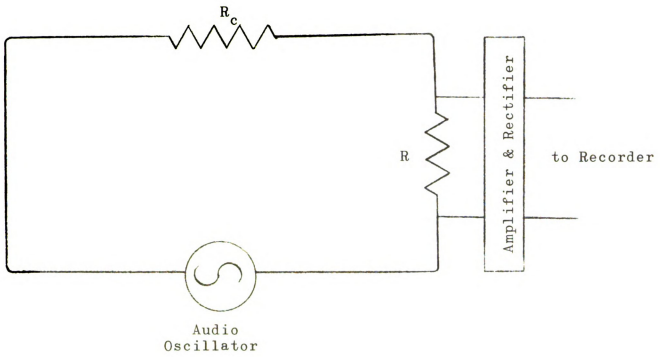

Figure 9. Electrical Circuit for Conductance Measurements

A variable frequency audio oscillator was used as the voltage source. The A. C. voltage across R was amplified, rectified, and measured with a Sargent multirange recorder. A schematic diagram of the rectifying-amplifying circuit is shown in Figure 10.

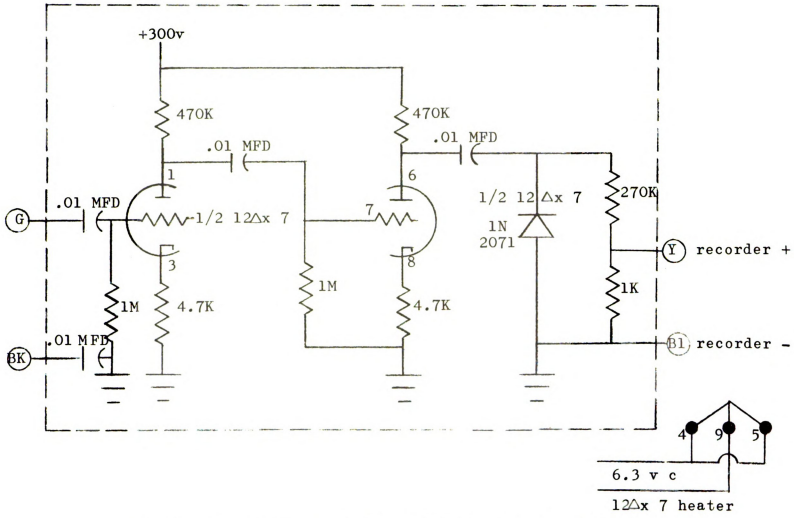

Figure 10. Schematic of Rectifying Amplifying Circuit

EXPERIMENTAL PROCEDURE

In-Vivo Experiments

Large mongrel dogs were anesthetized by intravenous injection of sodium pentobarbital (30 mg/Kg) and ventilated with a mechanical respirator. The gracilis muscle in the right hindlimb was surgically exposed. The main artery or two main arteries perfusing the muscle and the main vein or two main veins draining the muscle were isolated and collateral flow to the muscle was abolished by including all other structures except the nerves in a tourniquet. The alternate surgical procedures are illustrated in Figure 11. The gracilis muscle preparation has been previously described in detail.[29] The left femoral artery was ligated and a constant displacement blood pump was interposed between the proximal segment of the femoral artery and the hemodialyzer. Sodium heparin (5 mg/Kg) was injected intravenously as an anticoagulant. Initially, the dialyzer was filled with isotonic saline to prevent air emboli from entering the muscle. This saline was discarded and did not enter the gracilis. Blood leaving the dialyzer entered the gracilis muscle and the blood flow rate was adjusted so that the perfusion pressure was at or slightly above systemic pressure. Inlet and outlet dialyzer pressure as well as perfusion pressure and systemic pressure were monitored continuously on a direct writing Sanborn oscillograph. Four pressure

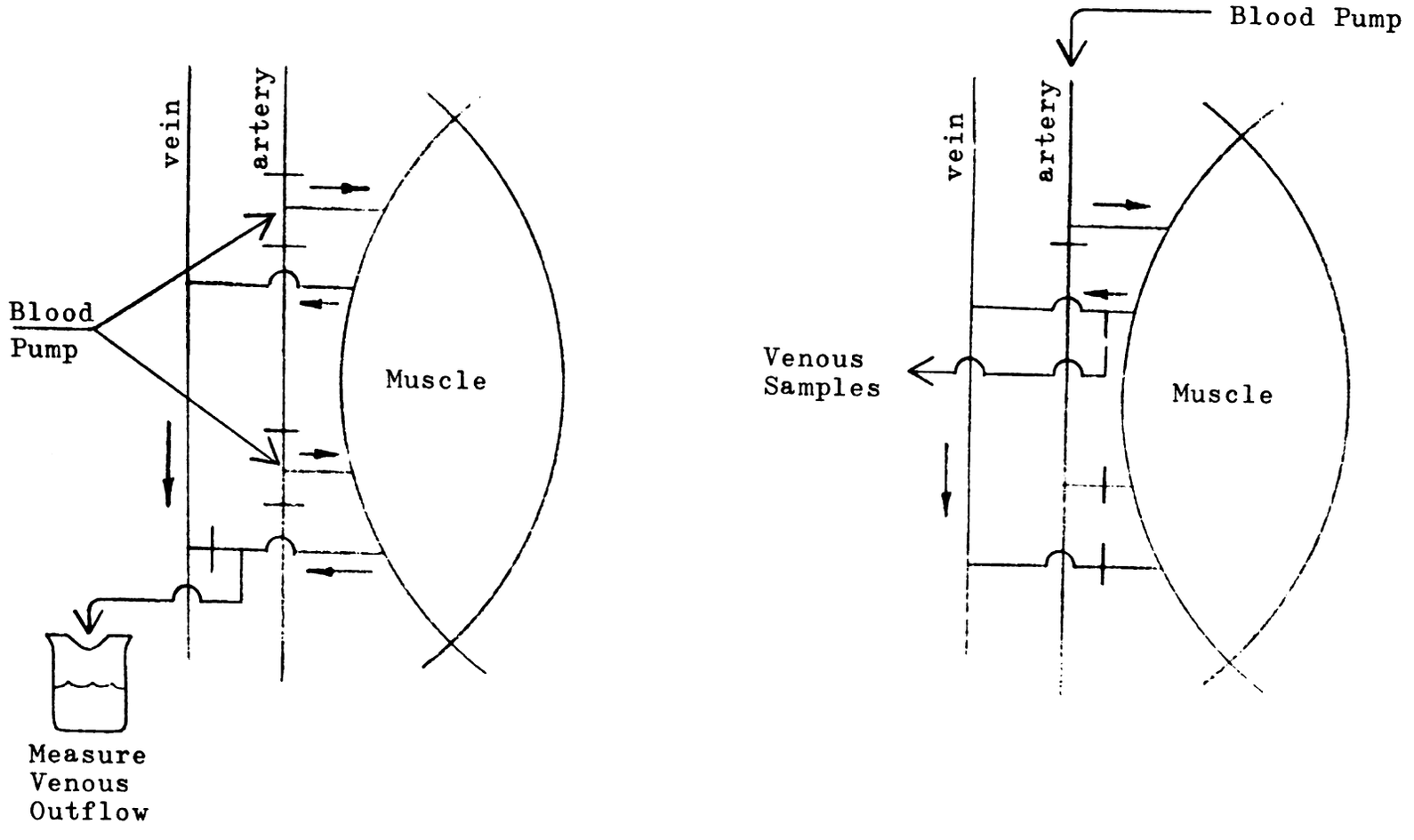

Figure 11. Alternate Surgical Procedures

transducers were used, all tubes and needles being flushed periodically with heparinized saline.

Blood concentration changes were achieved by using two dialysate solutions, a control or Ringer's solution containing approximately the normal concentrations of the major cations and anions in blood plasma (see Figure 8) and another in which the 4 meq/l of potassium ion was replaced by an identical amount of sodium. The control solution was designed to have little effect on blood pH, plasma osmolarity, and plasma ion concentrations. The zero potassium dialysate should then act identically to the control solution except that a gradient for the diffusion of potassium out of the blood is established. Both solutions were maintained at 37°C.

The gracilis muscle was perfused with blood dialyzed against the control solution until all pressures were steady and then by means of a simple valving arrangement the control solution was changed to zero potassium dialysate. Dialysate and blood flow circuits are illustrated in Figure 12. After a new steady state had been reached, blood samples were drawn from the blood entering the dialyzer, the blood entering the gracilis muscle (that is, the blood leaving the dialyzer), and the venous blood leaving the gracilis. These samples were analyzed for plasma potassium with a Beckman flame photometer. Osmolarity, pH, and hematocrit were checked periodically. The experimental procedure consisted of several such alternate dialyses.

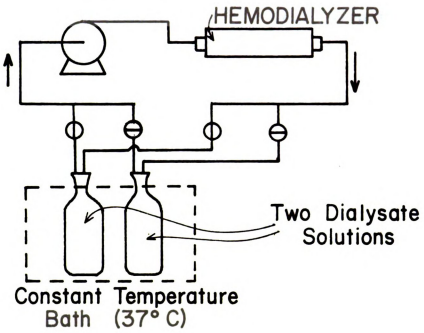

(a) Dialysate Circuit

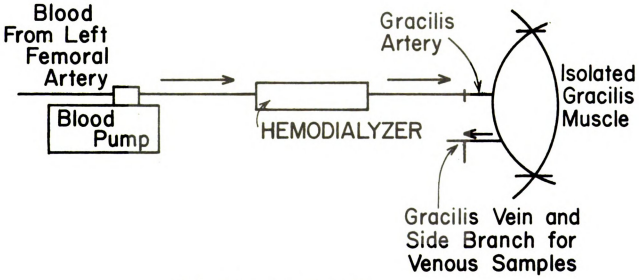

(b) Blood Circuit

Figure 12. Dialyzer Flow Circuits

The procedure also included challenging the muscle for an extended period of time, one hour, with the zero potassium dialysate to determine if the acute response of the potassium deficient muscle was modified with respect to the same response following short periods of hypokalemia.

Response to a Step Change in Dialysate Composition

A step change in dialysate concentration does not, of course, produce a step change in dialyzer outlet blood concentration. Rather the concentration falls approximately exponentially after a period of no change during which the blood in the outlet header and connecting tubing is being displaced. The plasma potassium concentration leaving the dialyzer rapidly approaches a steady state depending on the flow rate and hold up volume in the dialyzer and connecting tubing.

It is not possible to continuously monitor the potassium concentration of the blood leaving the dialyzer following a change in dialysate composition. It is necessary to analyze samples taken periodically. A minimum sample size of about 2 cm^3 for a flame photometric analysis makes this an ineffective procedure when the plasma potassium concentration is changing rapidly.

Thus, a series of laboratory experiments were run using a dilute KCl solution, 8 meq/l, as the "blood" side fluid. Two dialysate solutions were used, 8 meq/l KCl and distilled water. The use of dilute KCl made it

possible to continuously monitor "blood" concentration with a continuous flow conductivity cell (as described in Apparatus). Over the range of concentrations considered, the conductivity of aqueous KCl solutions is linear with respect to concentration as is shown in Figure 13. The un-steady state response to a step change in dialysate concentration was measured at various blood flow rates with a very high dialysate flow rate (greater than 500 ml/min).

Potassium Transport Model

The experiment designed to measure the acute response to local hypokalemia by alternately dialyzing against two dialysate solutions was not compatible with an experiment designed to verify a model for the transport of potassium in skeletal muscle. Perfusion with hypokalemic blood removed potassium from the muscle which was then partially or totally returned when the muscle was perfused with control blood. Thus, a series of experiments were conducted which were simply a long term potassium depletion of the muscle. The surgical procedure was the same as that for the previously described in-vivo experiments.

The isolated gracilis muscle of the anesthetized dog was perfused at constant flow rate with blood dialyzed against the control Ringer's solution. The blood flow rate was adjusted so that the perfusion pressure was equal to systemic pressure. After achieving a steady state

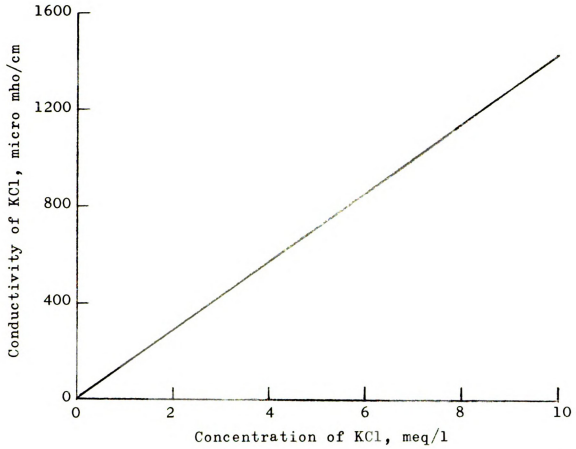

Figure 13. Conductivity of Dilute KCl Solutions [25]

under control conditions, the control dialysate was switched to zero potassium dialysate. Samples were then taken of the blood entering the gracilis muscle (that is, the blood leaving the dialyzer), and the venous blood leaving the gracilis at 5, 10, 30, 45, 60, 75, 90, 105, and 120 minutes after the switch of dialysate solutions. These samples were analyzed for plasma potassium with the Beckman flame photometer. The amount of potassium stripped from the muscle was determined by plotting venous and arterial potassium plasma concentrations versus time and graphically integrating the difference. The blood flow rate was determined after each experiment at the given pump setting using a stopwatch and graduated cylinder. Two blood samples were also analyzed for hematocrit so that the quantity $\frac{Q_B(1 - Hct)}{1000} \int_0^{120} (C_{ven} - C_{art})dt$ which is equal to the milliequivalents of potassium removed from the muscle could be calculated.

RESULTS AND DISCUSSION

The Acute Response

Figure 14 is a tracing of the acute response to hypokalemic blood from a typical experiment. The arrow indicates the point at which the dialysate was switched from Ringer's solution to zero potassium dialysate. Note the time lag, about one minute in this example, before the muscle was perfused with hypokalemic blood and the vascular resistance increased. Initially there was no rise in the perfusion pressure after switching dialysate sources since the gracilis muscle continued to be perfused with blood from the connecting tubing and outlet header of the hemodialyzer which was dialyzed against the control solution. After this period, hypokalemic blood entered the gracilis and the perfusion pressure increased to a new level. Systemic pressure remained unaffected. In this particular illustration, the potassium concentration of the plasma entering the muscle was reduced by 64% by dialyzing against the potassium-free solution. Blood flow rate was estimated to be 7.3 ml/min.

Figure 15 summarizes the results of all of the acute experiments, which have previously been reported.[32] Each point represents one gracilis muscle preparation and is an average value relative to control of several alternate responses to control and hypokalemic blood. The data from the one hour potassium depletion are not included in these results. For the range of plasma potassium

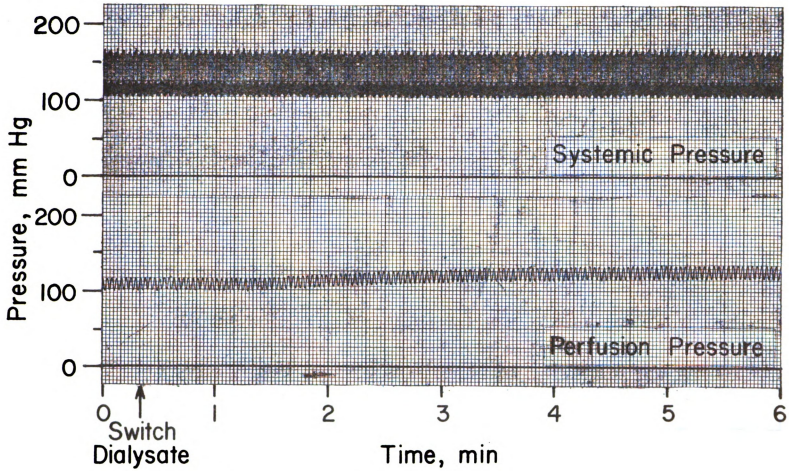

Figure 14. A Typical Acute Response

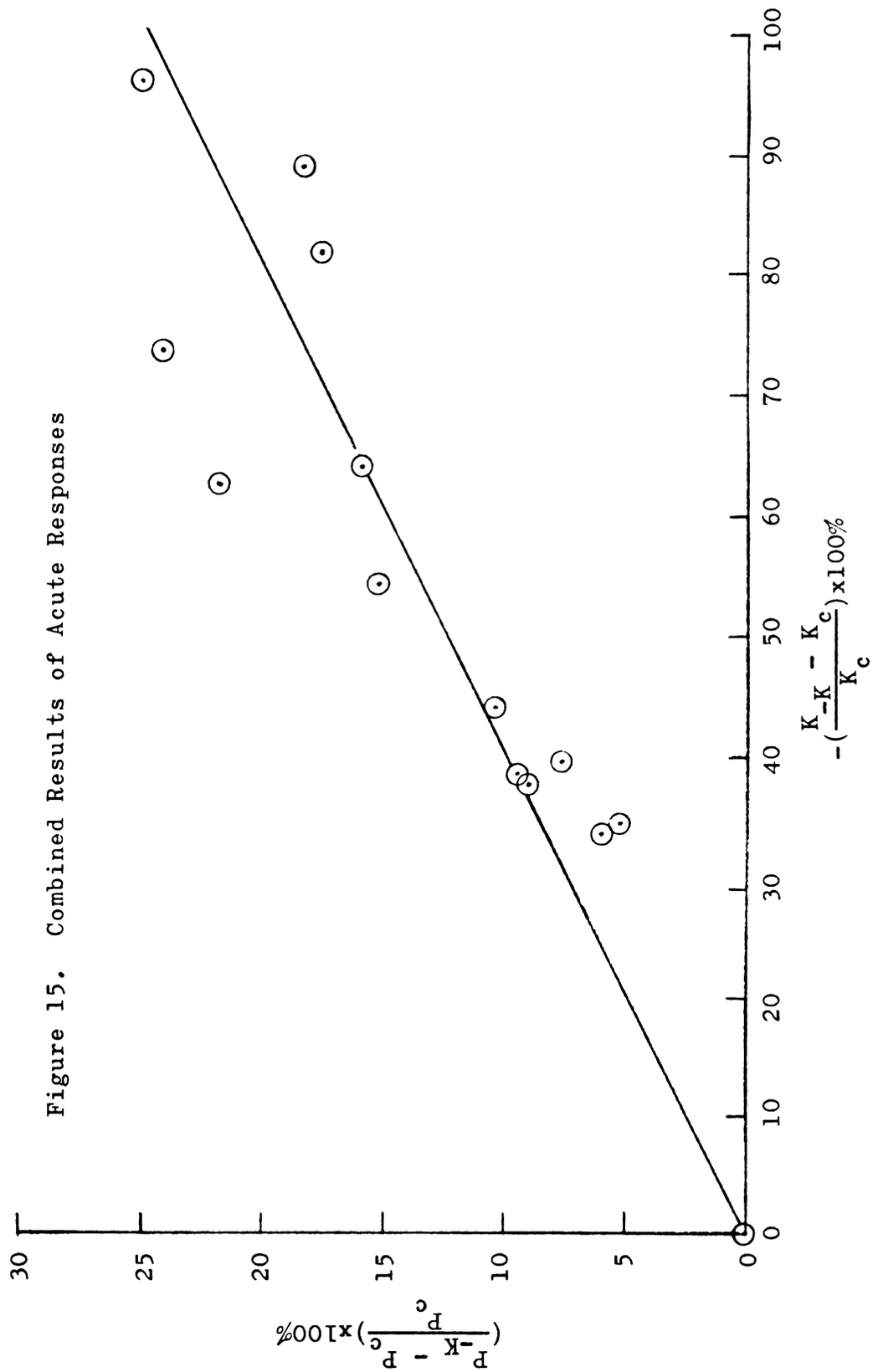

Figure 15. Combined Results of Acute Responses

concentrations considered, approximately 0.2 to 4.0 meq/l, the data can be represented by the straight line

$$(P_{-K} - P_c)/P_c = -0.25(K_{-K} - K_c)/K_c \qquad (13)$$

with a coefficient of correlation of 0.90. P_c and K_c refer to the perfusion pressure and plasma potassium concentration, respectively, when the blood is being dialyzed against the control solution. P_{-K} and K_{-K} refer to the perfusion pressure and plasma potassium concentration, respectively, when the blood is being dialyzed against the zero potassium dialysate. Thus, each point represents an increase in vascular resistance or perfusion pressure when switching from control to hypokalemic blood and a decrease in vascular resistance or perfusion pressure when switching from hypokalemic blood to control. No significant difference is obtained when these responses are plotted separately. Following one hour of perfusion with low potassium blood, the acute response, although present, was attenuated and modified with respect to that previously observed and, hence, these data were not included in Figure 15.

The Assumption of Constant Viscosity

The ultrafiltration characteristics of Cuprophane PT 150 are important since in addition to concentration differences across the membrane, pressure differences also exist. Ultrafiltration is the use of an elevated

pressure to drive liquids and other small particles through a semipermeable membrane. Switching to zero potassium dialysate raises the vascular resistance to flow and, hence, the pressure in the dialyzer also rises. Thus, it might be expected that the elevated pressure in the dialyzer would increase ultrafiltration, reduce the blood flow rate, and increase the hematocrit and viscosity, altering resistance in accordance with the Hagen-Poiseuille equation,

$$\Delta P/Q = R = (8/\pi)x(\mu)x(\ell/r^4). \qquad (1)$$

Henderson, Besareb, Michaels, and Bluemle[24] report an ultrafiltration rate for Cuprophane of $0.18x10^{-2}$ ml/min/cm^2 at 15 psi and room temperature. Their studies on other membranes suggest that the corresponding value for plasma would be considerably less. Since the ultrafiltration rate is directly proportional to the pressure difference across the membrane,[3,24,30] ultrafiltration rates for the two dialyzers used in this study (ultrafiltration areas of approximately 200 and 1000 cm^2) would be expected to be about $4.8x10^{-2}$ and $2.4x10^{-1}$ ml/min, respectively, for an average pressure difference across the membrane of 100 mm Hg.

The increase in the viscous component of resistance can be calculated by using Figure 16 which is a plot of hematocrit versus viscosity. The blood flow rates to the gracilis varied from about 5 to 25 ml/min. A maximum

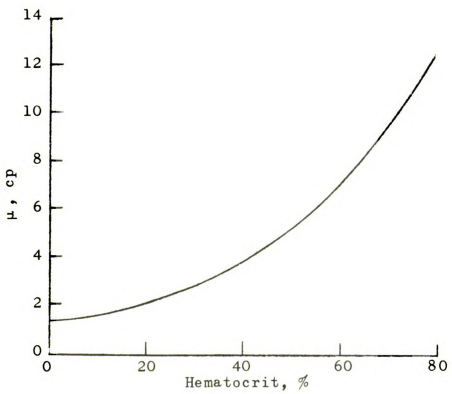

Figure 16. Viscosity versus Hematocrit[9]
(Viscosity measured in a large bore tube.)

value for the increase in viscosity and decrease in blood flow rate caused by passing blood through the dialyzer can be obtained by calculating the increase in hematocrit using the lowest blood flow rate, 5 ml/min, and the highest ultrafiltration rate, 2.4×10^{-1} ml/min, and assuming the blood entering the dialyzer has a hematocrit of 45%. The values thusly obtained are an increase in hematocrit from 45 to 47.3% and a decrease in blood flow rate from 5 to 4.76 ml/min. The corresponding values which result when the control Ringer's is switched to zero potassium dialysate can also be calculated by using the same flow rate and initial hematocrit and assuming the average blood side pressure in the dialyzer increases 25% or 25 mm Hg. Hence, the ultrafiltration rate increases 25% from 2.4×10^{-1} to 3.0×10^{-1} ml/min. These figures predict an increase in hematocrit from 45 to 47.9% and a decrease in blood flow rate from 5 to 4.70 ml/min.

The change in the viscous component of the blood entering the gracilis muscle as calculated from Figure 16, using hematocrits of 47.3 and 47.9%, is too slight to be read accurately and is probably compensated for by the slight reduction in flow rate to the gracilis from 4.76 to 4.70 ml/min. It should be reemphasized that the ultrafiltration rates quoted here are for water and not for blood and for this reason are undoubtedly higher than those which actually occur. In conclusion, the increase in viscosity and the decrease in flow rate are both small

and tend to cancel each other so that no correction has been made in Figure 15 and the increase in resistance is assumed to be totally the result of vascular constriction.

Conductivity Measurements

Typical results from the conductivity experiments using 8 meq/l KCl as a "blood" side fluid and distilled water as a dialysate are illustrated in Figure 17. The arrow at time zero indicates the dialysate is switched from 8 meq/l KCl to distilled water. Following a time delay during which blood in the outlet "blood" header is displaced, the conductivity of the "blood" fluid decreases to a steady-state.

Comparison of a normalized acute vascular response to hypokalemia from an in-vivo experiment with a normalized response to a step change in dialysate concentration from a conductivity measurement as in Figure 18, indicates that the constriction of the muscle follows closely the reduction of potassium by the dialyzer. The in-vivo response is from Experiment No. 9 and was calculated from the change in perfusion pressure. The responses to a step change in dialysate composition were obtained using a dilute KCl solution and the previously described conductivity cell at the "blood" outlet. In the absence of being able to monitor both vascular resistance and potassium concentration continuously in the same experiment, it is difficult to make an accurate comparison.

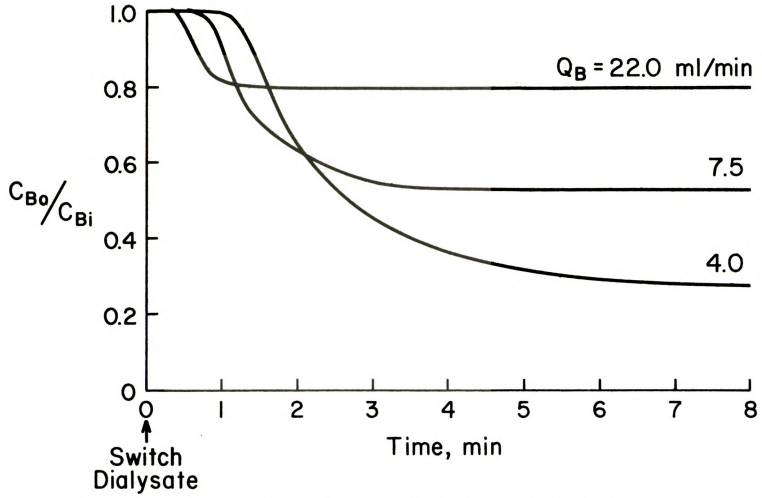

Figure 17. "Blood" Concentration Response to a Step Change in Dialysate Concentration

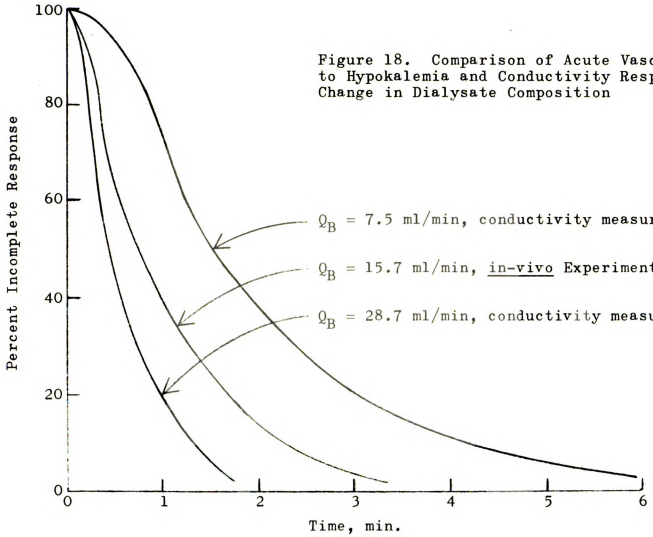

Figure 18. Comparison of Acute Vascular Response to Hypokalemia and Conductivity Response to a Step Change in Dialysate Composition

Hemodialyzer Efficiency

The optimum height of the blood channel can be calculated as recommended by Grimsrud and Babb[17]

$$a = 1.6 \sqrt[3]{h_o \mu \ell L / \Delta P_{max}} \quad (14)$$

and

$$1/h_o = 1/P + 0.5a/\mathcal{D}. \quad (9)$$

Equation (14) is slightly modified from Babb's equation to account for the length of the transfer area and the length of the blood channel not necessarily being equal. Since h_o is a function of a, the solution of the above equations requires trial and error.

For the dialyzers used in this study:

$1/P$ = 17 min/cm for KCl through Cuprophane PT 150 at 37°C and

22 min/cm for KCl through Cuprophane PT 150 at 25°C

$\mathcal{D}$ = 2.4×10^{-5} cm^2/sec for KCl/blood at 37°C and

1.9×10^{-5} cm^2/sec for KCl/water at 25°C

μ = 4.0×10^{-2} dyne-sec/cm^2 for blood and

0.9×10^{-2} dyne-sec/cm^2 for dilute KCl/water

ℓ = 10 cm (small dialyzer), 25 cm (large dialyzer)

L = 20 cm (small dialyzer), 35 cm (large dialyzer)

ΔP_{max} = 30,000 dynes/cm^2

The optimum half channel heights calculated from these values are 0.9×10^{-2} and 1.4×10^{-2} cm for the small and large dialyzer, respectively, at 37°C. The corresponding values at 25°C are 0.55×10^{-2} and 0.88×10^{-2} cm.

The choice of ΔP_{max} is rather arbitrary when using a blood pump but was kept small in these experiments to avoid puncturing or tearing of the Cuprophane PT 150 membranes. Since blood leaving the dialyzer is pumped into the arterial system of the vascular bed, average pressures in the hemodialyzer tend to be higher in this study than in artificial kidney use when the blood is returned to the venous system. Normal operating procedure for the artificial kidney is to suck the dialysate through the dialyzer so that the membranes do not collapse and offer abnormally high resistance to blood flow. In an effort to reduce the pressure difference across the membrane, the dialysate was pushed through the foam metal, thereby resulting in positive pressures on the dialysate side. The multiple dialysate delivery system includes the hardware necessary to easily make the conversion from positive to negative pressures on the dialysate side. Positive pressures were also used on the dialysate side for the conductivity measurements. In this case it was necessary to place a constriction at the blood outlet in order to maintain a pressure approximately equal to arterial pressure and sufficient

to keep the membranes spread and avoid channeling of the "blood" side fluid.

Comparison of Theoretical with Actual Efficiency

An experimental value of the overall mass transfer coefficient can be calculated from

$$h_o = (Q_B/A)\ln(C_{Bi}/C_{Bo}). \quad (15)$$

The transfer areas of the dialyzers are approximately 200 and 1000 cm^2. A correction could be made to account for the partial screening of the membrane by the foam metal support. The calculated and experimental values of the overall transfer coefficients are summarized in Table I. The values at 37°C are calculated from the results of the in-vivo experiments while those at 25°C are from the laboratory experiments using dilute KCl. It should be noted that there is some variability in the experimental values, h_o falling off markedly at low blood flow rates. For this reason the reported experimental values of h_o are averages of values obtained over the approximate range of flow rates, 5 to 25 ml/min.

Kiil dialyzers using Cuprophane membranes typically operate with an average overall resistance to mass transfer, based on the log mean concentration difference, of 100 min/cm.[17] Due to the inadequacies of the membrane support, this figure is very dependent on blood flow rate and blood pressure.

temp, °C	h_o, cm/min small dialyzer	h_o, cm/min large dialyzer
25	1/42, (1/24.4)	1/75, (1/25.9)
37	1/27, (1/20.2)	1/47, (1/21.9)

Table I.

Comparison of Theoretical and Experimental Values of the Overall Mass Transfer Coefficient (Theoretical values in parentheses)

Potassium Transport Model

The combined results of the previous experiments have demonstrated that the acute local response to hypokalemia is constriction and that the increase in vascular resistance follows closely in time the concentration of potassium in the blood leaving the dialyzer and entering the muscle. A new steady state for the vascular resistance is reached at the same time the blood concentration entering the muscle reaches a steady state (see Figure 18). Yet blood samples of the arterial and venous blood indicate that potassium is being continuously removed from the muscle as it is perfused with hypokalemic blood even though the local vascular response has reached a steady state. This is further motivation to seek a description of the transfer of potassium between the various vascular compartments of the gracilis muscle.

The results of the two hour potassium depletion experiments are summarized in Table II.

Exp. No.	C_{art}, meq/l	Hct, %	Q_B, ml/min	K removed, meq	k_cA_c, ml/min/100 g tissue
20	0.925	37.0	15.8	1.19	7.3
22	0.30	43.5	9.0	0.83	10.1
23	1.82	42.0	24.4	1.38	24.8
24	0.44	46.0	14.0	1.61	47.8
25	0.39	49.5	5.6	0.42	8.1

Table II.

Experimental Results for the Verification of the Transport Models

Both the two-compartment and three-compartment models were discussed under Theory. The two-compartment model is much easier to handle since it involves only two ordinary differential equations and one resistance to mass transfer. The three-compartment model involves two ordinary differential equations, one partial differential equation, and two resistances to mass transfer. As will be shown by comparing the results of both models, the controlling resistance lies in the muscle cell walls and not the capillary walls.

The three-compartment model involves fewer assumptions, so it was decided to fit the experimental values for the five two-hour potassium depletion experiments using this model and varying the parameter k_cA_c. It is

not possible, at least with these experiments, to separate the product. The three equations were solved numerically using the analog computer (Applied Dynamics AD 4). The mass balance for the blood compartment is a partial differential equation, and since analog computers can integrate with respect to only one independent variable, the x-dimension was discretized. Details of the solution of this model are given in Appendix I. Basically, the procedure was as follows: A particular value of the product $k_c A_c$ was chosen and the value of the integral

$$I = \int_0^{120\ \text{min}} (C_{ven} - C_{art})dt \qquad (16)$$

was computed for each of the boundary conditions, C_{art}, i.e., the concentration of the hypokalemic blood leaving the dialyzer and entering the muscle, as given in Table II. This procedure was repeated for several values of the product $k_c A_c$ and a plot of $k_c A_c$ versus the value of the integral was prepared. The values of the product $k_c A_c$ which fit the experimental data to the three-compartment model were read off this plot and are presented in the last column of Table II.

That the product $k_c A_c$ is not more constant is perhaps surprising. The two-compartment model used by Bell, Curtis, and Babb[4] as discussed in the section on Background was used to describe the exchange of urea between one compartment consisting of blood and interstitial fluid, and a

second compartment consisting of the cells. The following data were reported:

patient	wt, Kg	k_cA_c, liter/hr	k_cA_c/wt, liter/hr/Kg
1	44.7	33.1	0.694
2	51.0	15.5	0.304
3	22.5	24.8	1.102
4	71.7	44.0	0.614

Table III.

Results of a Study by Bell, Curtis, and Babb[4] for the Transfer of Urea

If the area for mass transfer is assumed to be roughly proportional to the patient's weight, k_cA_c/wt could be expected to be an indication of how reliable it is to assume a constant mass transfer coefficient from one patient to another. As can be seen, there is considerable variation in the parameter.

Some of the variation in the product k_cA_c is undoubtedly due to the presence of arteriovenous shunts which short-circuit the capillary system, the site of nutritive exchange between blood and tissue. Due to the variation in k_cA_c, the median value of 10.1 ml/min/100 g tissue was chosen as being representative and was used to calculate the variations in plasma, interstitial, and cell potassium concentrations with time. Figure 19 is a plot of $C_B(x)$,

Figure 19. Results of the Three-Compartment Model for C_{art} = 2.0 meq/l

C_i, and C_c versus time for the boundary condition C_{art} = 2 meq/l. The results of the three-compartment model indicate that the plasma is very nearly in equilibrium with the interstitial fluid by the time it leaves the capillaries. This suggests that the two-compartment model, which combines the plasma and interstitial compartments, should prove to be adequate.

The two-compartment model consists of two coupled, linear, ordinary differential equations which can be solved analytically by the method of Laplace transforms. Details are given in Appendix I. The results of the two-compartment model for the same boundary condition of C_{art} = 2 meq/l and same representative value of $k_c A_c$ = 10.1 ml/min/100 g tissue are presented in Figure 20. It will be noted that the results are similar to those of the three-compartment model. This model essentially neglects the resistance to transfer of potassium across the capillary wall in comparison to the resistance across skeletal muscle cells and, hence, predicts slightly higher mass transfer rates than the three-compartment model.

It should be noted that both models assume a step change is made in C_{art} at time zero, but the dialyzer does not produce a step change experimentally. This is an approximation which should only influence the results of the model for short times. Tabulated data from both models for various values of C_{art} are presented in Appendix I.

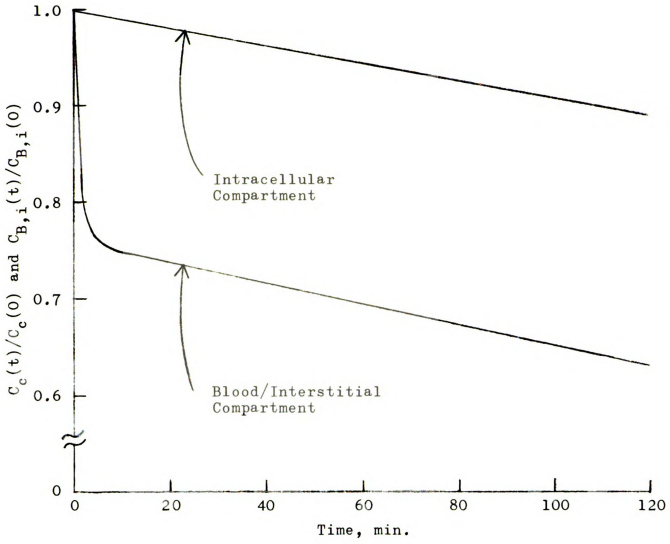

Figure 20. Results of the Two-Compartment Model for C_{art} = 2.0 meq/l

At the end of some experiments, both gracilis muscles were surgically removed and their weights compared. Some variation in the weight of the muscles from a given animal is to be expected, but on the average (see Appendix II) the increased weight of the experimental muscle can be attributed to filtration from the vascular to the extravascular compartments. This is a minor consideration in the compartmental mass balances as can be seen by considering the filtration of 10 ml of hypokalemic plasma (2 meq/l, for example). This would add only 0.02 meq of potassium to the muscle, a rather small amount when compared to the potassium removed by two hours of hypokalemic perfusion as given in Table II.

Renkin[31] measured the clearance of K^{42} from blood in the gracilis and gastrocnemius muscles of the dog. He considered an almost infinite "sink" for potassium existed in the cells, thereby minimizing back-diffusion and enabling him to consider the flux into the cells only. Renkin's model assumed two compartments representing total blood volume and extravascular volume. The compartments are separated by a barrier of area A with permeability coefficient P. Blood flows past the diffusion barrier at rate Q_B and the extravascular space is assumed homogeneous with respect to the diffusing material. The governing equation is then

$$\text{Clearance} = Q_B(1 - e^{-PA/Q_B}). \qquad (17)$$

Values of the product PA were reported as 7 $\pm$ 3 ml/min/100 g tissue. High values were associated with muscles of low vascular resistance. Clearly, values of the permeability-transfer area product must be evaluated in terms of the experimental procedure used.

The movement of ions may result from passive forces (concentration and potential gradients) and/or active transport. A mathematical expression for the flux due to the potential gradient requires specifying the potential and the concentration of the specific solute at each point in the membrane. Hence, a model of the membrane is needed. An equation for active transport presents similar problems in that it requires a mathematical representation or model. A straight line relationship, $C_c = mC_i + b$, was assumed in this study to relate intracellular and interstitial potassium concentrations. Thus, the simplifying assumption is that the net flux due to passive and active forces is directly proportional to a driving force which is a linear combination of the intracellular and extracellular concentration. It is obvious, then, that the value of the permeability-transfer area product, PA or $k_c A_c$, depends on the choice of driving force (m and b, in this instance) so that the results must be interpreted in this light.

The Resistance Mechanism

The acute local vascular response to potassium deficient blood as determined in this study is constriction

and increased resistance to blood flow. Elevation of the plasma potassium concentration to levels less than twice the normal value of 4 meq/l produces arteriolar dilation, while the acute local effect of a large excess of plasma potassium (greater than approximately 14 meq/l) is constriction.[33]

The above observations for small increases and decreases in potassium concentration are not in accord with the classical Nernst equation. A decrease in the ratio of interstitial to intracellular potassium should hyperpolarize the membrane and produce dilation. Similarly, an increase in this ratio should depolarize the membrane with a resultant constriction. Many investigators have reported results with isolated strips which are consistent with this classical concept. Bohr,[8] for example, reported that the effect of an increase in potassium concentration on smooth muscle is normally an increase in tension and, conversely, in a potassium free solution smooth muscle contractility decreases. On the other hand, Grundfest[18] challenged frog muscle fibers with hyperosmotic NaCl solutions in both the presence and absence of potassium. The cell membrane was found to be effectively impermeable to NaCl with potassium present in the bathing medium, but permeable to NaCl in the absence of potassium. The entry of NaCl into the muscle fibers was accompanied by the movement of water into the cells, swelling, and fiber depolarization.

However, in this study, the effect of low K in the presence of a normal Na concentration was not investigated.

The present study included challenging the muscle with a hypertonic solution during both the control and low K phases of the experiment. Both hypertonic NaCl and urea (1.03 ml/min of a 900 mosm solution) were infused into the blood leaving the hemodialyzer. The response to the hyperosmotic blood was identical in the control and low K phases of the procedure.

The seeming conflict in results between *in vitro* and *in vivo* studies is evidence that the mechanism by which vascular resistance is altered is complicated. The results of the present study are clear, however. The acute local vascular response to hypokalemia, as measured in the gracilis muscle of the anesthetized dog, is constriction and increased resistance to blood flow. Clearly, this area deserves more attention.

CONCLUSIONS

The Acute Response

The acute local vascular response to hypokalemia as produced by a non-dilution technique is constriction and increased vascular resistance. Furthermore, the relationship between percent change in plasma potassium concentration and percent change in vascular resistance appears to be linear, resistance increasing about 12½% for a 50% reduction in potassium ion concentration. The constriction follows closely the reduction of potassium by the dialyzer, as demonstrated in Figure 18. Both models suggest that the acute vascular response to hypokalemia is accompanied by a rapid decrease in the interstitial concentration of potassium, followed by the gradual reduction of the potassium concentration in the skeletal muscle cells. If these results can be extended to the smooth muscle in the walls of the arterioles, then the acute response corresponds to an alteration in the potassium concentration of the cell environment rather than the cell contents.

Hemodialyzer Efficiency

Examination of Table I indicates that the efficiency of the large dialyzer was considerably less than that of the small dialyzer, illustrating the fundamental difficulty of scaling up equipment while trying to maintain the same performance. The flow rate per unit width of

the blood channel was less in the large dialyzer than in the small dialyzer probably promoting channeling and uneven distribution of the flow. Thus, designing a dialyzer to remove a large percentage of a blood solute presents difficulties since this requires a low flow rate through the dialyzer.

Potassium Transport Model

Comparison of Figures 19 and 20 or the data in Appendix I indicates that both the two- and three-compartment models are adequate for describing potassium transport in muscle. The two-compartment model neglects the resistance to mass transfer across the capillary wall and, hence, predicts somewhat higher rates of mass transfer. The two-compartment model may not necessarily be adequate to describe the transport of other blood solutes as can be seen by examination of the following literature values.[26]

Solute	Capillary Wall PA, ml/min/100 g muscle	Blood-Tissue PA, ml/min/100 g muscle
Sucrose	18	5 - 11
Urea	54	4 $\pm$ 2

Table IV.
The Permeability Characteristics of Sucrose and Urea

Values of the permeability-area product, PA, for the capillary wall were calculated from Renkin's formula, Equation (17). Thus, urea appears similar to potassium in that the main barrier to diffusion is not the capillary wall, but probably the cell membrane in the tissue. Sucrose, on the other hand, which accumulates primarily in the interstitial fluid, would probably require a three-compartment model to adequately describe its distribution and exchange in muscle, since a major portion of the resistance to mass transfer is located in the capillary wall.

RECOMMENDATIONS

Vascular Effects of Ions

Haddy et al.[21] used a dilution technique to reduce ion concentrations and reported that more marked constriction occurs with combinations of local hypokalemia, hypercalcemia, alkalosis, and hypomagnesemia than with any one of the abnormalities alone. It is recommended that the present study be expanded to include hypomagnesemia, singly and in combination with hypokalemia. Hypercalcemia and alkalosis can be achieved by a simple infusion procedure and the dialysis technique developed in this study is of no particular advantage for studying these abnormalities singly.

Neither of the vascular models investigated in this study included a compartment for the vascular smooth muscle cells. It is these cells which are involved in the constrictor mechanism and the results of the transport models indicate that a change in cell potassium environment accompanies the acute response. It would seem reasonable to expand this study to include the effects of local hypokalemia on vascular smooth muscle composition. This would necessitate developing a new experimental procedure for sampling this compartment and developing an analytical method which is sensitive and yet does not require a large sample size. Neutron activation analysis might be ideally suited as an analytical technique.

Hemodialyzer Design

Under typical operating conditions, about 80% of the total resistance to mass transfer in a Kiil dialyzer (for urea) lies in the blood film.[17] Thus, development of a membrane with a greater permeability to urea would do little to increase the removal of urea from the blood. It was this observation which led Babb and Grimsrud to seek a better membrane support, one which would enable the thickness of the blood film to be controlled to within narrow limits. Nickel foam metal is excellent for this purpose but is not without its disadvantages. It is relatively rough and much more likely to puncture or tear the dialysis membranes than is the Kiil support. This is a particular concern for clinical use. Also, any deformation or indentation of the foam is permanent and can only be removed by milling the entire surface. And since the foam is initially only 1/8 inch thick, there is a limit to the amount which can be milled from the surface. Thus, if an open cell foam, probably made from a polymeric material which possesses some degree of resiliency and yet can be milled, could be developed, it would probably find clinical use as well as experimental use.

APPENDIX I

APPENDIX I

Derivation of Three-Compartment Model

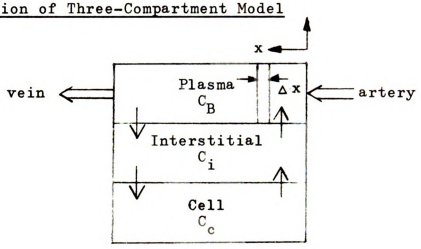

(1) Mass Balance for Plasma Compartment:

In - Out = Accumulation

$$(1 - Hct)Q_B C_B\Big|_x - (1 - Hct)Q_B C_B\Big|_{x+\Delta x} + k_B \pi D \Delta x (C_i - C_B) = \frac{\Delta[(1 - Hct)C_B \Delta x \pi D^2/4]}{\Delta t}.$$

Passing to the limit as Δt and Δx approach zero and noting that $\pi D^2/4 = V_B/\ell$ and $\pi D = A_B/\ell$ yields

$$\frac{\partial C_B}{\partial t} + \frac{Q_B \ell}{V_B}\frac{\partial C_B}{\partial x} = \frac{k_B A_B}{V_B(1 - Hct)}(C_i - C_B). \qquad (A\text{-}1)$$

(2) Mass Balance for the Interstitial Compartment:

In - Out = Accumulation

$$\sum_{x=0}^{\ell} k_B \pi D \Delta x (C_B - C_i) - k_c A_c (C_i - C_c/m + b/m) = \frac{\Delta(V_i C_i)}{\Delta t}.$$

Passing to the limit as Δt and Δx approach zero and noting that $\pi D = A_B/\ell$ yields

$$\frac{dC_i}{dt} = \frac{k_B A_B}{V_i} \frac{1}{\ell} \int_0^{\ell} (C_B - C_i)dx + \frac{k_c A_c}{V_i} \left(\frac{C_c}{m} - \frac{b}{m} - C_i\right). \quad \text{(A-2)}$$

(3) Mass Balance for the Intracellular Compartment:

In - Out = Accumulation

$$k_c A_c \left(C_i - \frac{C_c}{m} + \frac{b}{m}\right) = \frac{\Delta (V_c C_c)}{\Delta t} .$$

Passing to the limit as Δt approaches zero yields

$$\frac{dC_c}{dt} = \frac{k_c A_c}{V_c} \left(C_i - \frac{C_c}{m} + \frac{b}{m}\right). \quad \text{(A-3)}$$

Assumptions:

(A) Plug flow in capillaries.

(B) All mass transfer between blood and tissue takes place in capillaries.

(C) No exchange of potassium between plasma and red blood cells.[12, 30]

(D) Interstitial and intracellular compartments are perfectly mixed.

(E) Equilibrium conditions between intracellular potassium and interstitial potassium can be represented by $C_c = mC_i + b$.

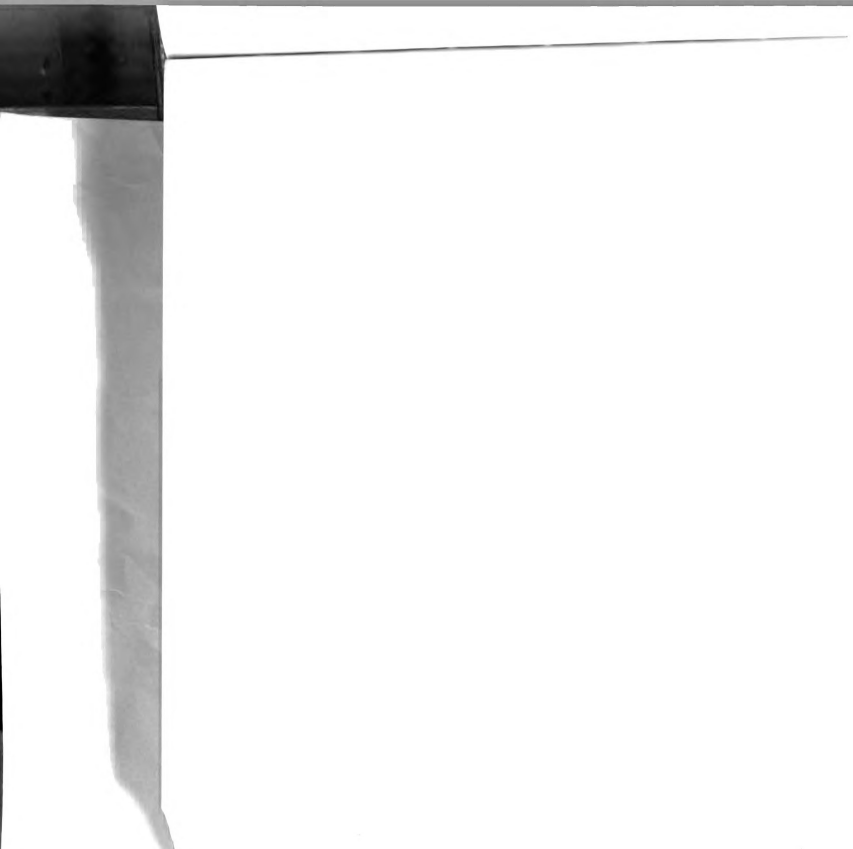

Derivation of Two-Compartment Model

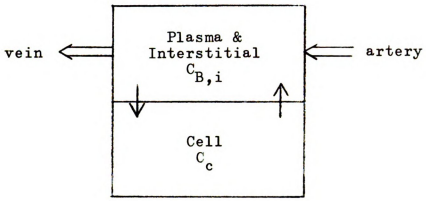

(1) Mass Balance for Plasma/Interstitial Compartment:

In - Out = Accumulation

$$(1 - Hct)Q_B C_{art} - (1 - Hct)Q_B C_{B,i} + k_c A_c\left(\frac{C_c}{m} - \frac{b}{m} - C_{B,i}\right) = \frac{\Delta[C_{B,i}V_i + C_{B,i}(1 - Hct)V_B]}{\Delta t} .$$

Passing to the limit as Δt approaches zero yields

$$\frac{dC_{B,i}}{dt} = \frac{(1 - Hct)Q_B}{V_B(1 - Hct) + V_i}(C_{art} - C_{B,i}) + \frac{k_c A_c}{V_B(1 - Hct) + V_i}\left(\frac{C_c}{m} - \frac{b}{m} - C_{B,i}\right) . \qquad (A-4)$$

(2) Mass Balance for the Interstitial Compartment:

In - Out = Accumulation

$$k_c A_c\left(C_{B,i} + \frac{b}{m} - \frac{C_c}{m}\right) = \frac{\Delta(V_c C_c)}{\Delta t} .$$

Passing to the limit as Δt approaches zero yields

$$\frac{dC_c}{dt} = \frac{k_c A_c}{V_c} \left(C_{B,i} + \frac{b}{m} - \frac{C_c}{m}\right) . \qquad \text{(A-5)}$$

Assumptions:

(A) All mass transfer between blood and tissue takes place in capillaries.

(B) No exchange of potassium between plasma and red blood cells.[12,30]

(C) Both compartments are perfectly mixed.

(D) Equilibrium conditions between intracellular potassium and interstitial potassium can be represented by $C_c = mC_i + b$.

Calculation of Coefficients for the Two- and Three-Compartment Models

The coefficients appearing in the two- and three-compartment model equations are:

$$A = \ell Q_B/V_B$$

$$B = k_B A_B/V_B(1 - Hct)$$

$$D = k_B A_B/V_i$$

$$E = k_c A_c/V_i$$

$$F = k_c A_c/V_c$$

$$G = Q_B(1 - Hct)/[V_B(1 - Hct) + V_i]$$

$$H = k_c A_c/[V_B(1 - Hct) + V_i]$$

$$J = k_c A_c/V_c$$

Representative values for the coefficients not involving $k_c A_c$ can be calculated from the following numbers which are available in the literature:

Capillary length = 0.1 cm[9]

Capillary diameter = 0.0008 cm[9]

Capillary blood velocity = 0.04 cm/sec[9]

Hematocrit = 45%

$V_c/V_i = 1.92$[19]

$V_B/V_i = 0.029$[19]

$k_B A_B$ = 90 ml/min/100 g tissue[31]

Capillary surface area = 7000 cm^2/100 g skeletal muscle[26]

Density of each compartment = 1 g/cm^3 (approximation)

Using the above values, although they are admittedly only representative values, the coefficients can be determined as

$$A = 2.40 \text{ cm/min}$$

$$B = 117 \text{ min}^{-1}$$

$$D = 1.87 \text{ min}^{-1}$$

$$E/F = 1.92$$

$$G = 0.37 \text{ min}^{-1}$$

$$H/J = 1.89$$

Analog Solution for Three-Compartment Model

The differential equations and boundary conditions will be restated with the vascular compartments designated by 1, 2, and 3 instead of B, i, and c.

$$\frac{\partial C_1}{\partial t} = -A\frac{\partial C_1}{\partial x} + B(C_2 - C_1) \tag{A-6}$$

$$\frac{dC_2}{dt} = \frac{D}{\ell}\int_0^{\ell}(C_1 - C_2)dx + E(\frac{C_3}{m} - \frac{b}{m} - C_2) \tag{A-7}$$

$$\frac{dC_3}{dt} = F(C_2 - \frac{C_3}{m} + \frac{b}{m}) \tag{A-8}$$

$$\frac{dI}{dt} = C_1(t, \ell) - C_1(t,0) \tag{A-9}$$

The boundary conditions are

$C_1(0,x) = 4$ meq/l

$C_1(t,0) = C_{11}$

$C_2(0) = 4$ meq/l

$C_3(0) = 155$ meq/l

$I(0) = 0$ meq-min/l

I, when multiplied by the plasma flow rate, represents the amount of potassium stripped from the muscle. This quantity was used as a criterion for fitting the model to experimental data.

Analog computation was chosen as the method of solution of the above equations. Analog computers can integrate

with respect to only one independent variable so the x-dimension was discretized. Due to equipment limitations, the number of x increments was chosen as 7.

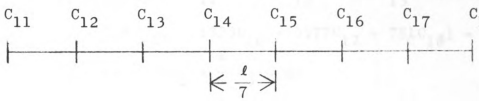

Figure 21. Division of Capillary Length into Increments

The use of 3-point derivative formulas for the x-partial in equation (A-6) yields

$$\frac{dC_{1i}}{dx} = \frac{C_{1i+1} - C_{1i-1}}{2\ell/7}, \quad i = 2, 3, \ldots 7 \tag{A-10}$$

$$\frac{dC_{18}}{dt} = \frac{C_{16} - 4C_{17} + 3C_{18}}{2\ell/7} \tag{A-11}$$

The integral expression in equation (A-7) can be simplified by use of a closed Newton-Cotes formula[38] for equally-spaced increments. The result is

$$\frac{D}{\ell}\int_0^{\ell} C_1 dx = \frac{D}{17280}(751C_{11} + 3577C_{12} + 1323C_{13} + 2989C_{14} + 2989C_{15} + 1323C_{16} + 3577C_{17} + 751C_{18}) \tag{A-12}$$

The equations can be summarized as

$$\frac{dC_{1i}}{dt} = -A\left(\frac{C_{1i+1} - C_{1i-1}}{2\ell/7}\right) + BC_2 - BC_{1i}, \quad i = 2, 3, \ldots 7 \tag{A-13}$$

$$\frac{dC_{18}}{dt} = -A\left(\frac{C_{16} - 4C_{17} + 3C_{18}}{2\ell/7}\right) + BC_2 - BC_{18} \qquad \text{(A-14)}$$

$$\frac{dC_2}{dt} = \frac{D}{17280}(751C_{11} + 3577C_{12} + 1323C_{13} + 2989C_{14} + 2989C_{15} + 1323C_{16} + 3577C_{17} + 751C_{18}) - (D + E)C_2 + \frac{E}{m}(C_3 - b) \qquad \text{(A-15)}$$

$$\frac{dC_3}{dt} = FC_2 - \frac{F}{m}(C_3 - b) \qquad \text{(A-16)}$$

$$\frac{dI}{dt} = C_{18} - C_{11} \qquad \text{(A-17)}$$

The following substitutions are made in order to properly scale the variables:

$$C'_{1i} = C_{1i}/4, \; i = 1, 2, \ldots 8$$

$$C'_2 = C_2/4$$

$$C'_3 = C_3/4m - b/4m$$

$$I' = I/S$$

Also, the magnitude of the coefficients of the concentrations must be such that their absolute value is less than or equal to 1.6. This can be accomplished by making the substitution $\tau = Bt$, where τ is machine time, t is real time, and B is the largest of the coefficients. Furthermore, real time t will be divided by 100 to make 120 minutes system time equal to 1.2 (or 120 volts) on the analog. The final equations, with $\alpha = 7A/2B\ell$, become

$$\frac{dC'_{1i}}{dt} = \alpha C'_{1i-1} - \alpha C'_{1i+1} + C'_2 - C'_{1i}, \quad i = 2, 3, \ldots 7 \tag{A-18}$$

$$\frac{dC'_{18}}{dt} = -\alpha C'_{16} + 4\alpha C'_{17} - 3\alpha C'_{18} + C'_2 - C'_{18} \tag{A-19}$$

$$\frac{dC'_2}{dt} = \frac{D}{17280B}(751C'_{11} + 3577C'_{12} + 1323C'_{13} + 2989C'_{14} + 2989C'_{15} + 1323C'_{16} + 3577C'_{17} + 751C'_{18}) - (\frac{D + E}{B})C'_2 + \frac{E}{B}C'_3 \tag{A-20}$$

$$\frac{dC'_3}{dt} = \frac{F}{mB}C'_2 - \frac{F}{mB}C'_3 \tag{A-21}$$

$$\frac{dI'}{dt} = \frac{4}{BS}(C'_{18} - C'_{11}) \tag{A-22}$$

It is these equations which were programmed on the Applied Dynamics AD 4 analog computer. The analog program is shown in Figure 22 with the potentiometer settings in Table V.

Using this program, the experimental data from each of the two-hour potassium depletion experiments was fit by picking a value for the coefficient k_cA_c/V_c, which was denoted by F in the three-compartment model and by J in the two-compartment model, and computing the value of the integral I for each of the boundary conditions. This was done for several values of k_cA_c/V_c and from a plot of k_cA_c/V_c versus I, the value corresponding to the

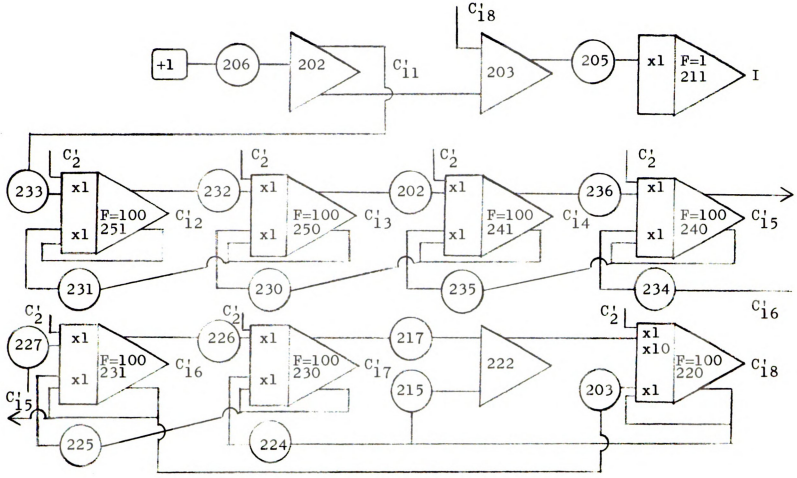

Figure 22. Analog Program for Solution of Three-Compartment Model

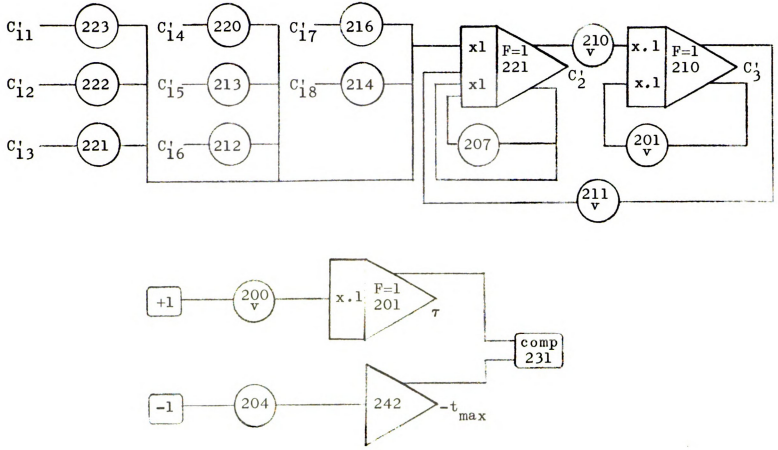

Figure 22. Analog Program for Solution of Three-Compartment Model (cont.)

Potentiometer Number	Value	Input	Output
200	10/B	+1 ref	201
201	1000F/mB	210^-	210
202	α	250^+	241
203	α	231^-	220
204	$t_{max}/100$	-1 ref	242
205	400/BS	203^+	211
206	C'_{11}	+1 ref	202
207	[100(D+E)/B] - 1	221^-	221
210	1000F/mB	221^+	210
211	100E/B	210^+	221
212	1323 β	231^+	221
213	2989 β	240^+	221
214	751 β	220	221
215	0.3 α	220^-	222
216	3577 β	230^+	221
217	0.4 α	230^+	222
220	2989 β	241^+	221
221	1323 β	250^+	221
222	3577 β	251^+	221
223	751 β	202^+	221
224	α	220^-	230
225	α	230^-	231
226	α	231^+	230
227	α	240^+	231
230	α	241^-	250
231	α	250^-	251
232	α	251^+	250
233	α	202^+	251
234	α	231^+	240
235	α	240^-	241
236	α	241^+	240

Table V.

Potentiometer Settings for Analog Solution
($\alpha = 7A/2B\ell$ and $\beta = 100D/17280B$)

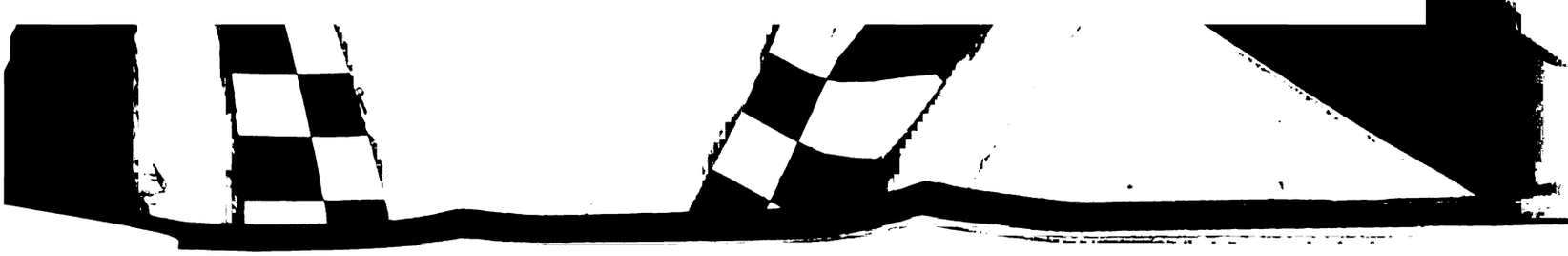

experimental value of I was determined. This plot is shown for Experiment No. 22 in Figure 23. By assuming that 76.25% of the total muscle weight is water and that 62.5% of this water is intracellular,[19] then intracellular water is 50.1% of the muscle by weight. Using this value as an estimate of V_c, $k_c A_c$ in ml/min/100 g tissue was computed for each experiment. It is these values which are presented in Table II.

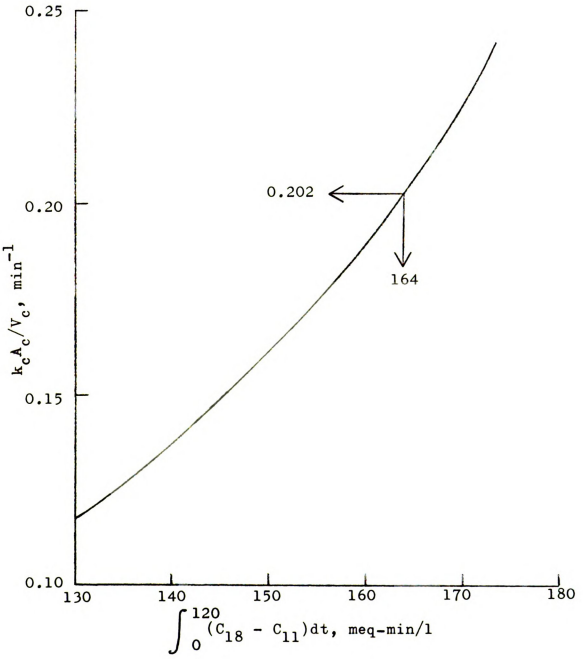

Figure 23. Determination of k_cA_c

t, min.	$C_{11}=C_{art}$	C_{12}	C_{13}	C_{14}	C_{15}	C_{16}	C_{17}	$C_{18}=C_{ven}$	$\int_0^t (C_{ven}-C_{art})dt$	C_2	C_3
0	0.00	4.00	4.00	4.00	4.00	4.00	4.00	4.00	0.00	4.00	155.0
1	0.00	1.42	2.16	2.54	2.74	2.85	2.91	2.93	3.36	2.96	154.9
2	0.00	1.16	1.78	2.09	2.26	2.35	2.39	2.42	6.00	2.44	154.6
3	0.00	1.04	1.59	1.87	2.02	2.10	2.14	2.16	8.26	2.18	154.3
4	0.00	0.98	1.49	1.76	1.90	1.97	2.01	2.03	10.32	2.05	154.0
5	0.00	0.95	1.44	1.70	1.83	1.90	1.94	1.96	12.30	1.98	153.6
10	0.00	0.90	1.36	1.60	1.73	1.80	1.83	1.85	21.66	1.87	151.8
20	0.00	0.85	1.29	1.52	1.64	1.70	1.74	1.75	39.62	1.77	148.3
30	0.00	0.80	1.22	1.44	1.56	1.62	1.65	1.66	56.58	1.68	144.9
60	0.00	0.68	1.04	1.23	1.33	1.38	1.40	1.42	102.40	1.43	135.9
90	0.00	0.58	0.89	1.05	1.13	1.17	1.20	1.21	141.36	1.22	128.3
120	0.00	0.50	0.76	0.89	0.96	1.00	1.02	1.03	174.54	1.04	121.7

Table VI.
Tabulated Data from Three-Compartment Model for Various Boundary Conditions
(C_{art} = 0.0, concentrations in meq/l)

t, min.	$C_{11}=C_{art}$	C_{12}	C_{13}	C_{14}	C_{15}	C_{16}	C_{17}	$C_{18}=C_{ven}$	$\int_0^t (C_{ven}-C_{art})dt$	C_2	C_3
0	1.00	4.00	4.00	4.00	4.00	4.00	4.00	4.00	0.00	4.00	155.0
1	1.00	2.06	2.61	2.90	3.06	3.13	3.18	3.20	2.52	3.22	154.9
2	1.00	1.87	2.32	2.57	2.69	2.76	2.79	2.81	4.50	2.82	154.7
3	1.00	1.78	2.18	2.40	2.51	2.57	2.60	2.61	6.18	2.63	154.5
4	1.00	1.73	2.11	2.31	2.42	2.47	2.50	2.51	7.72	2.53	154.2
5	1.00	1.71	2.07	2.27	2.37	2.42	2.45	2.46	9.20	2.48	154.0
10	1.00	1.67	2.02	2.20	2.29	2.34	2.37	2.38	16.18	2.40	152.6
20	1.00	1.63	1.96	2.13	2.22	2.27	2.30	2.31	29.56	2.32	150.0
30	1.00	1.60	1.91	2.07	2.16	2.20	2.23	2.24	42.22	2.25	147.5
60	1.00	1.51	1.78	1.91	1.99	2.02	2.04	2.05	76.32	2.07	140.8
90	1.00	1.43	1.66	1.78	1.84	1.87	1.89	1.90	105.28	1.91	135.1
120	1.00	1.37	1.57	1.66	1.71	1.74	1.76	1.76	129.88	1.77	130.3

Table VI.
Tabulated Data from Three-Compartment Model for Various Boundary Conditions (cont.)
(C_{art} = 1.0, concentrations in meq/l)

t, min.	$C_{11}=C_{art}$	C_{12}	C_{13}	C_{14}	C_{15}	C_{16}	C_{17}	$C_{18}=C_{ven}$	$\int_0^t (C_{ven}-C_{art})dt$	C_2	C_3
0	2.00	4.00	4.00	4.00	4.00	4.00	4.00	4.00	0.00	4.00	155.0
1	2.00	2.70	3.07	3.26	3.37	3.42	3.45	3.46	1.68	3.47	154.9
2	2.00	2.58	2.88	3.04	3.12	3.16	3.19	3.20	2.98	3.21	154.8
3	2.00	2.52	2.78	2.93	3.00	3.04	3.06	3.07	4.10	3.08	154.7
4	2.00	2.48	2.74	2.87	2.94	2.97	2.99	3.00	5.12	3.01	154.5
5	2.00	2.47	2.71	2.84	2.90	2.94	2.96	2.97	6.08	2.98	154.3
10	2.00	2.44	2.67	2.79	2.85	2.89	2.90	2.91	10.70	2.92	153.4
20	2.00	2.42	2.63	2.75	2.81	2.84	2.86	2.86	19.50	2.87	151.7
30	2.00	2.40	2.60	2.71	2.77	2.79	2.81	2.81	27.84	2.83	150.1
60	2.00	2.33	2.51	2.60	2.65	2.67	2.69	2.69	50.24	2.70	145.7
90	2.00	2.28	2.43	2.51	2.55	2.57	2.58	2.58	69.16	2.59	141.9
120	2.00	2.24	2.36	2.43	2.47	2.48	2.49	2.50	85.18	2.50	138.8

Table VI.
Tabulated Data from Three-Compartment Model for Various Boundary Conditions (cont.)
(C_{art} = 2.0, concentrations in meq/l)

t, min.	$C_{11}=C_{art}$	C_{12}	C_{13}	C_{14}	C_{15}	C_{16}	C_{17}	$C_{18}=C_{ven}$	$\int_0^t (C_{ven}-C_{art})dt$	C_2	C_3
0	3.00	4.00	4.00	4.00	4.00	4.00	4.00	4.00	0.00	4.00	155.0
1	3.00	3.35	3.53	3.63	3.68	3.70	3.72	3.72	0.82	3.73	155.0
2	3.00	3.28	3.43	3.51	3.55	3.57	3.58	3.59	1.46	3.60	154.9
3	3.00	3.25	3.38	3.45	3.49	3.51	3.52	3.52	2.02	3.53	154.8
4	3.00	3.24	3.36	3.42	3.46	3.47	3.48	3.49	2.50	3.49	154.8
5	3.00	3.23	3.34	3.41	3.44	3.46	3.47	3.49	2.98	3.48	154.7
10	3.00	3.21	3.32	3.38	3.41	3.43	3.44	3.44	5.20	3.45	154.2
20	3.00	3.20	3.31	3.36	3.39	3.41	3.41	3.41	9.46	3.42	153.4
30	3.00	3.19	3.29	3.34	3.37	3.38	3.39	3.39	13.48	3.40	152.6
60	3.00	3.16	3.24	3.29	3.31	3.32	3.33	3.33	24.16	3.34	150.5
90	3.00	3.13	3.20	3.24	3.26	3.27	3.28	3.28	33.08	3.28	148.8
120	3.00	3.11	3.17	3.20	3.22	3.23	3.23	3.23	40.52	3.24	147.3

Table VI.
Tabulated Data from Three-Compartment Model for Various Boundary Conditions (cont.)
(C_{art} = 3.0, concentrations in meq/l)

Solution of Equations for the Two-Compartment Model

The two-compartment model consists of two coupled, linear, ordinary differential equations with boundary conditions at zero time. These can be transformed into two algebraic equations by the method of Laplace transforms and uncoupled to yield

$$\frac{\bar{C}_{B,i}}{C_B(0)} = \frac{p^2 + a_1 p + a_o}{(p - \lambda_1)(p - \lambda_2)p}$$

and

$$\frac{\bar{C}_c}{C_c(0)} = \frac{p^2 + b_1 p + b_o}{(p - \lambda_1)(p - \lambda_2)p}$$

where

$$\lambda_{1,2} = \frac{-G-H-J/m \pm \sqrt{G^2+2GH-2GH/m+2HJ/m+H^2+J^2/m^2}}{2}$$

$$a_1 = \frac{HC_c(0)+JC_{B,i}(0)+mGC_{art}-bH}{mC_{B,i}(0)}$$

$$a_o = \frac{GJC_{art}}{mC_{B,i}(0)}$$

$$b_1 = \frac{JmC_{B,i}(0)+GmC_c(0)+HmC_c(0)+bJ}{mC_c(0)}$$

$$b_o = \frac{mGJC_{art}+bGJ}{mC_c(0)}$$

The inverse transform can be found and, after considerable rearrangement, the solutions are:

$$C_{B,i}(t) = C_{art} - \left\{ \frac{\lambda_1^2 C_{B,i}(0) + \lambda_1 (HC_c(0)/m + JC_{B,i}(0)/m + GC_{art} - bH/m) + JGC_{art}/m}{-\lambda_1(\lambda_1 - \lambda_2)} \right\} \exp(\lambda_1 t)$$

$$+ \left\{ \frac{\lambda_2^2 C_{B,i}(0) + \lambda_2 (HC_c(0)/m + JC_{B,i}(0)/m + GC_{art} - bH/m) + JGC_{art}/m}{-\lambda_2(\lambda_1 - \lambda_2)} \right\} \exp(\lambda_2 t)$$

$$C_c(t) = mC_{art} + b - \left\{ \frac{\lambda_1^2 C_c(0) + \lambda_1 (JC_{B,i}(0) + GC_c(0) + HC_c(0) + bJ/m) + JGC_{art} + JGb/m}{-\lambda_1(\lambda_1 - \lambda_2)} \right\} \exp(\lambda_1 t)$$

$$+ \left\{ \frac{\lambda_2^2 C_c(0) + \lambda_2 (JC_{B,i}(0) + GC_c(0) + HC_c(0) + bJ/m) + JGC_{art} + JGb/m}{-\lambda_2(\lambda_1 - \lambda_2)} \right\} \exp(\lambda_2 t)$$

These equations were solved on the CDC 6500 digital computer using the program in Table VII.


```
      PROGRAM TWOCOM(INPUT,OUTPUT,TAPE 3=OUTPUT,TAPE 2=INPUT)
      REAL J, L1, L2, M, INT
      DIMENSION DT(3), XT(4)
      DATA DT/0.1,1.0,5.0/
      DATA XT/0.0,1.0,10.0,120.0/
      DATA G,H,J,B/0.376,0.382,0.202,79.4/
      DATA M,CBI,CCI/18.9,4.0,155.0/
  200 FORMAT (19X,1HT,18X,2HCB,18X,8HCC,17X,3HINT,17X,3HCBR,
     217X,3HCCR,/)
  300 FORMAT (8X,F12.6,8X,F12.6,8X,F12.6,8X,F12.6,8X,F12.6,
     28X,F12.6)
  400 FORMAT(1H2,9X,18HRESULTS FOR CART =,F10.4,///)
  500 FORMAT(5X,7E15.6)
      CART=0.0
      R1=G+H+J/M
      R2=SQRT(R1*R1-4.*G*J/M)
      L1=0.5*(R2-R1)
      L2=-0.5*(R2+R1)
    1 WRITE (3,400) CART
      WRITE (3,200)
      DO  6  I=1,3
      T=XT(I)
      R3=(H*(CCI-B)+J*CBI)/M + G*CART
      R4=CCI*(G+H) + J*(CBI+B/M)
      R5=J*G*(CART+B/M)
    2 EX1=-EXP(L1*T)/(L1*(L1-L2))
      EX2=-EXP(L2*T)/(L2*(L1-L2))
      R6=-(L1*L1*CBI + L1*R3 + L1*L2*CART)
      R7=L2*L2*CBI + L2*R3 + L1*L2*CART
      CB=CART + EX1*R6 + EX2*R7
      CC=M*CART + B - EX1*(L1*L1*CCI + L1*R4 + R5) + EX2*(L2*
     2L2*CCI + L2*R4 + R5)
      INT=R6*EX1/L1 + R6/(L1*L1*L1 - L1*L1*L2) + R7*EX2/L2 +
     2R7/(L2*L2*L1 - L2*L2*L2)
      CBR=CB/CBI
      CCR=CC/CCI
      WRITE (3,300) T,CB,CC,INT,CBR,CCR
      T=T + DT(I)
      IF(T-XT(I+1)) 2,2,6
    6 CONTINUE
      CART=CART + 0.5
      IF(CART - 4.0) 1,9,9
    9 END
```

Table VII.

Exact Solution for Two-Compartment Model

t, min.	$C_{B,i}$	C_c	$\int_0^t (C_{B,i}-C_{art})dt$
0	4.00	155.0	0.00
1	2.94	154.9	3.41
2	2.45	154.6	6.07
3	2.21	154.3	8.39
4	2.09	153.9	10.53
5	2.03	153.5	12.59
10	1.94	151.6	22.47
20	1.84	147.9	41.36
30	1.74	144.4	59.29
60	1.49	134.9	107.72
90	1.27	126.8	149.09
120	1.09	119.9	184.41

t, min.	$C_{B,i}$	C_c	$\int_0^t (C_{B,i}-C_{art})dt$
0	4.00	155.0	0.00
1	3.21	154.9	2.55
2	2.84	154.7	4.55
3	2.66	154.5	6.29
4	2.57	154.2	7.90
5	2.53	153.9	9.44
10	2.46	152.5	16.85
20	2.38	149.7	31.02
30	2.31	147.1	44.46
60	2.12	139.9	80.79
90	1.95	133.8	111.81
120	1.82	128.7	138.30

Table VII.

Tabulated Data from Two-Compartment Model for Various Boundary Conditions (C_{art} = 0.0 and 1.0, concentrations in meq/l)

t, min.	$C_{B,i}$	C_c	$\int_0^t (C_{B,i}-C_{art})dt$
0	4.00	155.0	0.00
1	3.47	154.9	1.70
2	3.22	154.8	3.04
3	3.11	154.6	4.19
4	3.05	154.5	5.27
5	3.02	154.3	6.30
10	2.97	153.3	11.23
20	2.92	151.5	20.68
30	2.87	149.7	29.64
60	2.75	145.0	53.86
90	2.64	140.9	74.54
120	2.54	137.4	92.20

t, min.	$C_{B,i}$	C_c	$\int_0^t (C_{B,i}-C_{art})dt$
0	4.00	155.0	0.00
1	3.74	155.0	0.85
2	3.61	154.9	1.52
3	3.55	154.8	2.10
4	3.52	154.7	2.63
5	3.51	154.6	3.15
10	3.49	154.2	5.62
20	3.46	153.2	10.34
30	3.44	152.4	14.82
60	3.37	150.0	26.93
90	3.32	147.9	37.27
120	3.27	146.2	46.10

Table VII.

Tabulated Data from Two-Compartment Model for Various Boundary Conditions (cont.)
(C_{art} = 2.0 and 3.0, concentrations in meq/l)

APPENDIX II

Exp. No.	Q_B, ml/min	$-(\frac{K_{-K} - K_c}{K_c})x100$	$(\frac{P_{-K} - P_c}{P_c})x100$	Dialyzer Size
1	13.0	44.0	10.3	small
2	-	64.0	15.8	small
3	8.4	62.5	21.8	small
4	19.0	33.3	5.85	small
6	15.2	38.5	9.35	small
7	16.2	37.5	8.9	small
9	15.7	39.5	7.9	small
10	20.5	34.2	5.2	small
11	8.6	54.2	15.2	small
12	13.5	73.6	24.2	large
13	8.5	81.6	17.6	large
14	7.9	96.0	25.1	large
14	12.4	89.0	18.35	large

Table IX.
Tabulated Results for the Acute Vascular Response

Exp. No.	Wt. of Control Muscle, g	Wt. of Experimental Muscle, g	Difference, g	Percent Inc. from Control
14	44.9	65.9	21.0	47
15	32.0	43.0	11.0	34
22	79.2	100.7	21.5	27
23	95.3	116.0	20.7	22
24	83.2	95.6	12.4	15
25	61.7	65.5	3.8	6
				Average = 25%

Table X.
Edema in <u>In-Vivo</u> Experiments

NOMENCLATURE

a - half channel height

A - area or coefficient in three-compartment model, $\ell Q_B/V_B$

b - equilibrium constant

B - coefficient in three-compartment model, $\frac{k_B A_B}{V_B(1-Hct)}$

C - concentration

D - coefficient in three-compartment model, $k_B A_B/V_i$

$\mathcal{D}$ - diffusivity

E - coefficient in three-compartment model, $k_c A_c/V_i$

$\mathcal{E}$ - voltage

F - coefficient in three-compartment model, $k_c A_c/V_c$

G - coefficient in two-compartment model, $\frac{Q_B(1-Hct)}{V_B(1-Hct)+V_i}$

h - mass transfer coefficient

H - coefficient in two-compartment model, $\frac{k_c A_c}{V_B(1-Hct)+V_i}$

Hct - hematocrit

i - current

I - value of the integral $\int_0^t (C_{ven}-C_{art})dt$

J - coefficient in two-compartment model, $k_c A_c/V_c$

k - permeability constant

K - potassium concentration

ℓ - length of capillary or of mass transfer area in dialyzer

L - total length of blood channel in dialyzer

m - equilibrium constant

p - Laplace transform variable

P - permeability constant or perfusion pressure

Δ P - pressure drop

Q - volumetric flow rate

r - capillary radius

R - resistance

S - integral scaling factor

t - time

U - velocity

V - volume

w - channel width

x - coordinate

y - coordinate

μ - viscosity

τ - machine time

Subscripts

art - arterial

B - blood

c - cell

D - dialysate

f - final

i - inlet, initial, interstitial

K - potassium

M - membrane

max - maximum allowable value

o - overall, outlet

T - total

ven - venous

LIST OF REFERENCES

LIST OF REFERENCES

1. Abel, J. J., L. G. Rountree, and B. B. Turner, J. Pharmacol. Exp. Therap., 5, 275(1913-4).

2. Babb, A. L., C. J. Maurer, D. L. Fry, R. P. Popovich, and R. E. McKee, Chem. Eng. Progr. Symposium Ser. No. 84, 64, 59(1968).

3. Baremberg, R. L., and J. E. Kiley, Trans. Amer. Soc. Artif. Int. Organs, 7, 9(1961).

4. Bell, R. L., F. K. Curtis, and A. L. Babb, Trans. Amer. Soc. Artif. Int. Organs, 11, 183(1965).

5. Bellman, R., R. Kalaba, and J. A. Jacquez, Bull. Math. Biophysics, 22, 181(1960).

6. Bischoff, K. B., and R. G. Brown, Chem. Eng. Progr. Symposium Ser. No. 66, 62, 33(1966).

7. Bloom, F., The Blood Chemistry of the Dog and Cat, Gamma Publications, Inc., New York, 1960, p. 128.

8. Bohr, D. F., Pharmacol. Rev., 16, 85(1964).

9. Burton, A. C., Physiology and Biophysics of the Circulation, Year Book Medical Publishers, Inc., Chicago, 1966.

10. Dedrick, R. L., and K. B. Bischoff, Chem. Eng. Progr. Symposium Ser. No. 84, 64, 32(1968).

11. Emerson, T. E., Jr., J. B. Scott, and F. J. Haddy, Fed. Proc., 27, 743(1968).

12. Frazier, H. S., A. Sicular, and A. K. Solomon, J. Gen. Physiol., 37, 631(1954).

13. Grimsrud, L., Ph.D. Thesis, University of Washington (1965).

14. Grimsrud, L., and A. L. Babb, Trans. Amer. Soc. Artif. Int. Organs, 10, 101(1964).

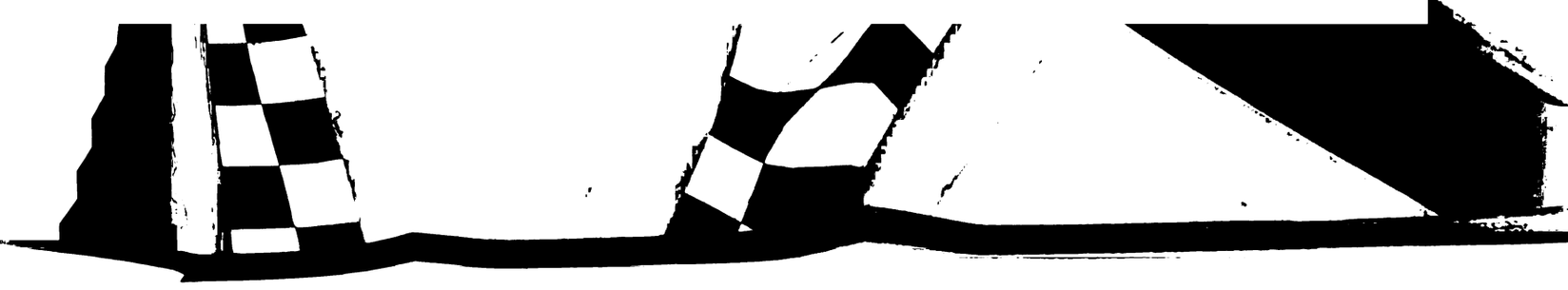

15. Grimsrud, L., and A. L. Babb, Trans. Amer. Soc. Artif. Int. Organs, 10, 31(1964).

16. Grimsrud, L., and A. L. Babb, Chem. Eng. Progr. Symposium Ser. No. 66, 62, 20(1966).

17. Grimsrud, L., and A. L. Babb, Biomechanical and Human Factors Symposium, 23(1967).

18. Grundfest, H., Fed. Proc., 26, 1613(1967).]

19. Guyton, A. C., Textbook of Medical Physiology, 3 ed., W. B. Saunders Co., Philadelphia, 1966.

20. Haddy, F. J., and J. B. Scott, in Electrolytes and Cardiovascular Disease, edited by E. Bajusz, Karger, White Plains, New York, 1965, p. 383.

21. Haddy, F. J., J. B. Scott, M. A. Florio, R. M. Daugherty, Jr., and J. N. Huizenga, Am. J. Physiol., 204, 202(1963).

22. Haddy, F. J., Supplement I to Circulation Research, 18 and 19, 14(1966).

23. Haddy, F. J., and J. B. Scott, Annual Review of Pharmacology, 6, 49(1966).

24. Henderson, L. W., A. Besareb, A. Michaels, and L. W. Bluemle, Jr., Trans. Amer. Soc. Artif. Int. Organs, 13, 216(1967).

25. Hodgman, C. D., ed., Handbook of Chemistry and Physics, 44th ed., The Chemical Rubber Publishing Co., Cleveland, 1963, p. 2695.

26. Landis, E. M. and J. R. Pappenheimer, in Handbook of Physiology, Section II: Circulation, edited by W. F. Hamilton and P. Dow, American Physiological Society, Washington, D. C., 1963, p. 961.

27. Leonard, E. F., and R. L. Dedrick, Chem. Eng. Progr. Symposium Ser. No. 84, 64, 15(1968).

28. Leonard, E. G., and L. W. Bluemle, Trans. Amer. Soc. Artif. Int. Organs, 8, 182(1962).

29. Nagle, F. J., J. B. Scott, B. T. Swindall, and F. J. Haddy, Am. J. Physiol., 214, 885(1968).

30. Pappenheimer, J. R., Physiol. Rev., 33, 387(1953).

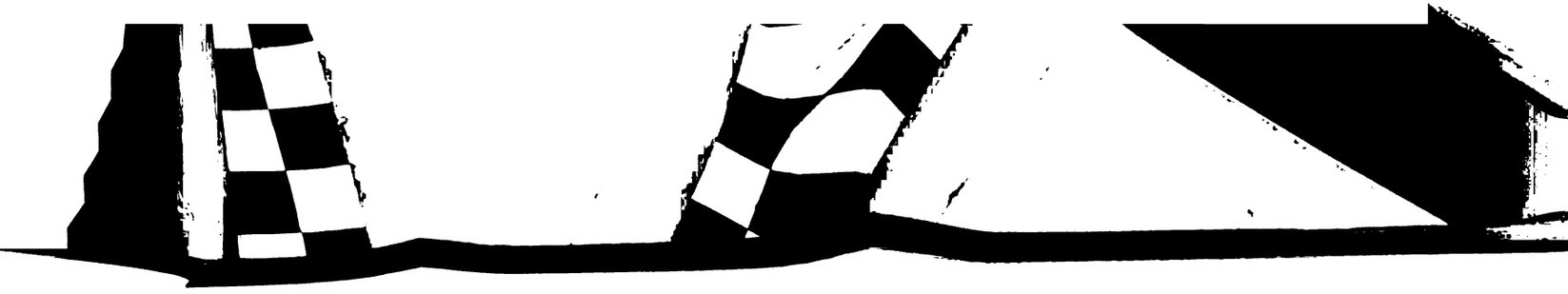

31. Renkin, E. M., Am. J. Physiol., 197, 1205(1959).

32. Roth, S. A., D. K. Anderson, D. P. Radawski, J. B. Scott, and F. J. Haddy, Physiologist, 12, 343(1969).

33. Scott, J. B., R. M. Daugherty, Jr., H. W. Overbeck, and F. J. Haddy, Fed. Proc., 27, 1403(1968).

34. Sheppard, C. W., W. R. Martin, and G. Beyl, J. Gen. Physiol., 34, 411(1951).

35. Vadot, L., Trans. Amer. Soc. Artif. Int. Organs, 10, 11(1964).

36. Van der Does de Bye, J. A. W., and J. Schenk, Appl. Sci. Res., A3, 308(1953).

37. Waddell, W. J., and R. G. Bates, Physiological Reviews, 49, 285(1969).

38. See for example: Abramowitz, M., and I. A. Stegun, eds., Handbook of Mathematical Functions, U. S. Dept. of Commerce, National Bureau of Standards, 1968, p. 886.